

Coordinated by



University of Vaasa  
VAASAN YLIOPISTO

Co-funded by

BUSINESS  
FINLAND



# Flexible Clean Propulsion Technologies

## 2<sup>nd</sup> Review Meeting

22-23 APRIL 2026

| VAASA (UNIVERSITY OF VAASA CAMPUS)

| CONFERENCE SUMMARY



University of Vaasa  
VAASAN YLIOPISTO



Åbo Akademi



Aalto University



LUT  
University



VTT



UNIVERSITY OF OULU



UNIVERSITY  
OF TURKU



Tampereen yliopisto  
Tampere University



WÄRTSILÄ



AGCO  
POWER



MEYER TURKU  
SHIPYARD 1727



PROVENTIA



rexroth  
A Bosch Company



NESTE



Lumikko



hycamite



MERIAURA

## FLEX-CPT 2ND REVIEW MEETING: Highlights and Perspectives

The Flexible Clean Propulsion Technologies (Flex-CPT) project marked a key point in its journey with the 2<sup>nd</sup> Review Meeting, held on 22–23 April 2026 at the University of Vaasa campus.

This conference summary presents selected highlights from the presentations, discussions, and posters shared during the event. The publication provides an overview of key insights, developments, and perspectives contributed by project partners and invited experts, reflecting the breadth of ongoing work within the Flex-CPT consortium.

As highlighted by Project Leader Prof. Maciej Mikulski in his welcome address, Flex-CPT is fundamentally about building the critical mass of competence, resources, and enabling solutions needed to respond to the complexity of a fuel-diversified future. With no single fuel or technological concept capable of addressing all sustainability challenges, the project brings together expertise across the marine and off-road sectors to develop solutions that are intrinsically fuel- and platform-agnostic. The strong participation in this review meeting reflected the consortium's shared commitment to that goal and to advancing a common vision for the future of clean propulsion technologies.

The meeting had two main objectives: first, to review Flex-CPT's intermediate milestones and progress toward securing an economically stable, zero-emission future for the Finnish powertrain industry in a fuel-diversified future; and second, to strengthen a forward-looking perspective on the off-road powertrain sector toward 2030 by assessing future targets, validating current solutions, and identifying areas requiring further R&D efforts.

Day 1 featured plenary sessions, including perspectives on the non-road mobile machinery user landscape, electrification challenges and opportunities from both manufacturer and supplier viewpoints, lessons that off-road applications can draw from road-vehicle powertrains, and policy measures to promote decarbonisation. The day concluded with a panel discussion titled *'What's next for the off-road powertrain sector?'*, bringing together senior experts from industry and academia to examine future targets, emerging challenges, technology development pathways, and research priorities shaping the future of off-road powertrains. Day 2 started with an inspiring visit to LOGSET, offering participants a valuable opportunity to explore state-of-the-art forest machine manufacturing and ongoing powertrain innovations. The visit strengthened the connection between Flex-CPT research and its industrial applications.

The programme then continued with technical sessions on multi-fuel engines and flexible powertrains, followed by a poster session. Together, these activities ensured that strategic direction and technical progress informed one another.

Our sincere thanks go to all speakers, session moderators, poster presenters, organizers, and participants for the effort and commitment that made this review meeting a meaningful milestone for Flex-CPT!

*Best Regards,*

**Prof. Maciej Mikulski**  
Project Leader, Flex-CPT

**Merja Kangasjärvi**  
Project Manager, Flex-CPT

**Diana Ibraheem**  
Communication Coordinator, Flex-CPT

## Programme – Day 1, Wednesday 22 April

11:30–13:00	<b>Registration (Levón Auditorium) and Lunch (Restaurant Mathilda)</b>
13:00–14:45	<p><b>PLENARY SESSION 1</b> Room: Levón Opening and Welcome (moderator)   Maciej Mikulski, UVA</p> <ol style="list-style-type: none"> <li><b>Non Road Mobile Machinery User Landscape</b> Timo Kokko, AGCO Power &amp; David Köping, AGCO Finland</li> <li><b>Off-Road Mobile Machinery Electrification – Challenges and Opportunities</b> <ul style="list-style-type: none"> <li><b>Machine Manufacturer</b>   Jonas Hedström, Logset</li> <li><b>System Supplier</b>   Arno Amberla, Proventia</li> </ul> </li> </ol>
14:45–15:45	<b>Coffee break (in front of Levón Auditorium, 1st floor)</b> <b>AGCO tractor show-off (yard in front of Tervahovi)</b>
15:45–17:15	<p><b>PLENARY SESSION 2</b> Room: Levón Moderator: Maciej Mikulski, UVA</p> <ol style="list-style-type: none"> <li><b>Lessons from Road Vehicle Powertrains for The Future Sustainable Off-Road Applications</b> Martin Tunér, Lund University, Sweden</li> <li><b>Policy Measures to Promote the Decarbonisation of Non-Road Mobile Machinery</b> Kaarina Kaminen, Finnish Environment Institute</li> </ol>
17:15–18:15	<p><b>PANEL DISCUSSION</b> Room: Levón Moderator: Maciej Mikulski, UVA</p>
19:30	<b>Dinner at the Restaurant Bacchus</b>

## Programme – Day 2, Thursday 23 April

8:45–11:00	<b>COMPANY VISIT: LOGSET</b> Bus transportation from the University of Vaasa and Vaasa City centre	
11:00–12:15	<b>Lunch (Restaurant Mathilda)</b>	
12:15–14:00	<p><b>TECHNICAL SESSION 1: MULTI-FUEL ENGINES</b> Room: Wolff   Moderator: Rasmus Pettinen, VTT</p> <ol style="list-style-type: none"> <li><b>NVO Fuel Injection for Low Load Extension of RCCI Combustion</b> Amir Soleimani &amp; Jacek Hunicz, UVA</li> <li><b>Adaptive Modelling &amp; on-Board Optimal Control of RCCI Combustion</b> Amir Talebi &amp; Mohammad Esfarjani, UVA</li> <li><b>Analysis of Hydrogen Engine Blowby Behavior: Simulation and Validation</b> Touraj Hashempour, UVA</li> <li><b>Towards HD SI methanol engine runs</b> Mayanka Jha, Aalto</li> </ol>	<p><b>TECHNICAL SESSION 2: FLEXIBLE POWERTRAINS</b> Room: Kurtén   Moderator: Mika Huuhtanen, UOULU</p> <ol style="list-style-type: none"> <li><b>Comparative Life-Cycle and Techno-Economic Assessment of Diesel, Battery-Electric and Hydrogen Pathway for Non-Road Mobile Machinery</b> Anthony Katumwesigye, ÅAU</li> <li><b>Comparative Well-To-Wake GHG Performance of Alternative Marine Fuels in Cruise Shipping Across LCA Frameworks</b> Ramtin Heydarian, ÅAU</li> <li><b>Large-Eddy Simulations of Droplet Size Effects in Early-Stage Urea-Water Spray Injection</b> Azher Haneef, Aalto</li> <li><b>Coolant Flow Modelling for Optimization of Thermal Management System Configurations</b> Lassi Puolakka, TAU</li> </ol>
14:00–14:30	<b>Coffee break (Restaurant Mathilda)</b>	
14:30–15:45	<b>POSTER SESSION</b> Room: C303	

# Plenary Sessions



# Non-road Mobile Machinery User Landscape – Power Unit Producer Point of View

**Author:** Timo Kokko, AGCO Power

The presentation began with an overview of AGCO Power’s future development areas for NRMM. There is no single solution for everything, and AGCO Power is focused on ICE (internal combustion engine) efficiency improvements, as well as developing and testing alternative-fuel capabilities. AGCO Power’s new CORE engine family is a base for the future. Research on new power unit concepts continues, and electrification is part of the development. Regulatory requirements and technology availability are key elements in defining future NRMM power source options.

## Future technology options for off-road machinery

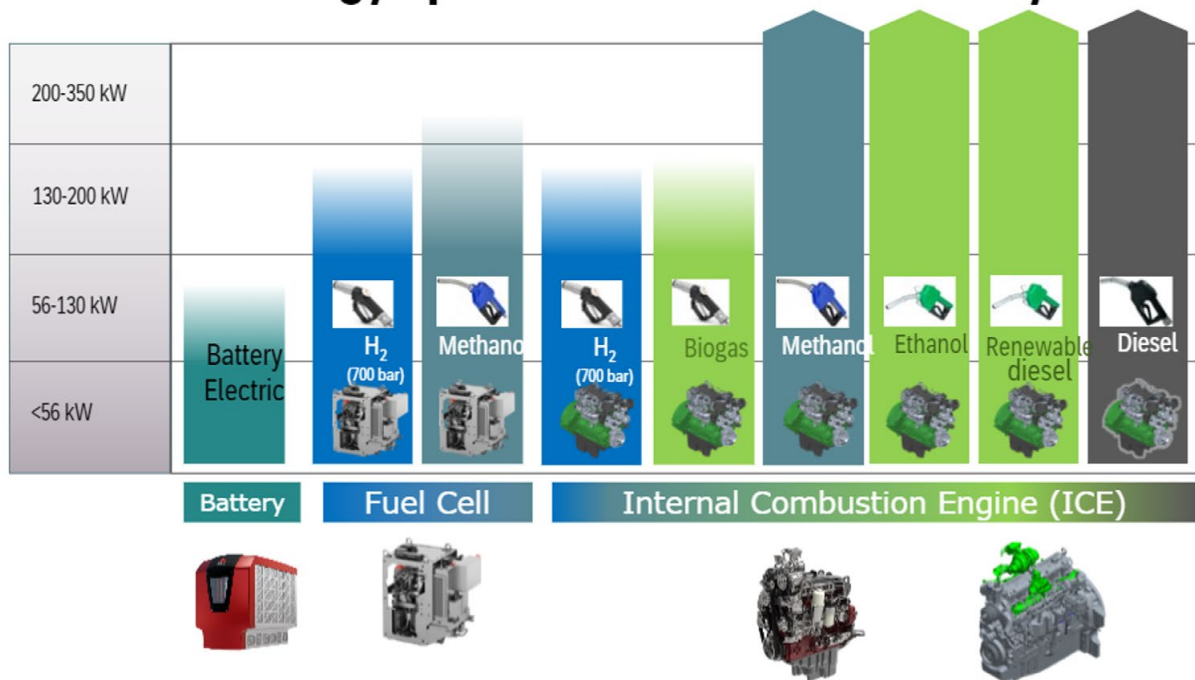


**Figure 1.** Future technology options for off-road machinery

Customer needs and success are central to AGCO Power’s development focus, including the following key points:

- Total cost of ownership
- Fuel availability and cost
- Vehicle performance and range
- Durability and residual value.

# Non-Road Mobile Machinery User Landscape – End-user Point of View

**Author:** David Köping, *AGCO Suomi*

This presentation summarizes the challenges, future development needs, and focus areas from an end-user perspective. Farm sizes are steadily increasing, and operating conditions are becoming more demanding. Farmers must complete the same field work within the same timeframe as before, but across a significantly larger number of hectares. Farm machinery must operate reliably, and the operating range must support a full day's work without significant interruptions.

From an end-user point of view, there are many important areas to focus when selecting new equipment, including:

- Dual-fuel options: If the same equipment can use alternative fuels with the same technology, it is a major benefit.
- Fuel availability and storage: Fuel should be easy and safe to store, cost-effective, and consistently available.
- TCO: Machine cost, maintenance cost, and fuel consumption are key elements.
- Usability and resale value: Manoeuvrability in the intended use case matters. Reliable machines retain value and are easier to resell than low-performing products.



Overall, the conclusion is that the transition in the NRMM user landscape toward cleaner propulsion machinery will be gradual and based on multiple technologies. While alternative fuels and electrification will grow in certain segments, customer value, cost-efficiency, and usability will ultimately determine which solutions succeed. AGCO Power and AGCO, as leading agricultural machinery producers, continue working toward clean propulsion technologies.

# Off-Road Mobile Machinery Electrification

Author: Jonas Hedström, LOGSET

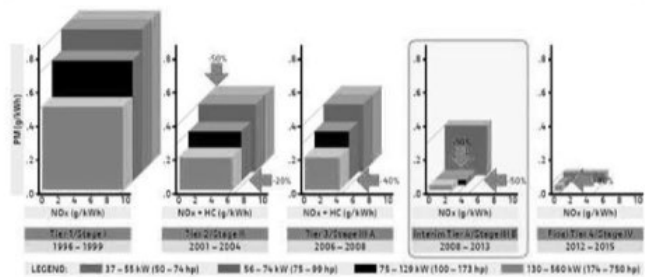
## Electrification development trigger @ Logset

The first emission regulation requiring DEF solution was Stage 4 Interim in 2011, Logsets largest CTL harvester, Logset 10H GT, was then discontinued due to low sales and complex DEF solution for 8,4 litre engines. The demand for larger harvesters picked up in 2014–15 but no reasonable alternative was found building a conventional diesel engine installation including DEF This was the starting point for squeezing more power out of the 7,4 litre engine, used in mid-sized harvesters, to equal or even higher maximum power output than in the previous 8,4 litre version

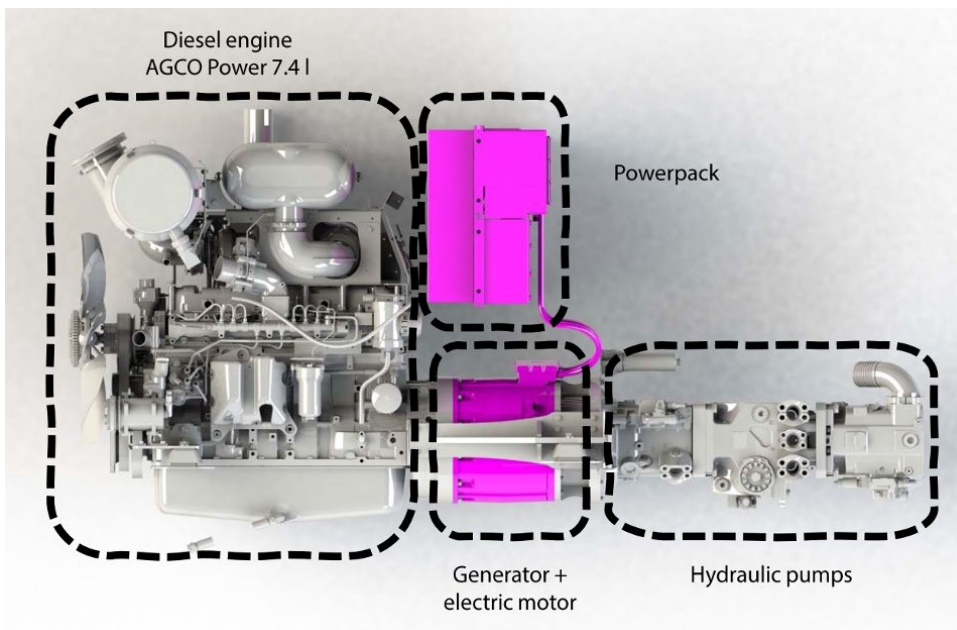
En världsnyhet från Kvevlax. Det låter osannolikt, men skogsmaskinsföretaget Logsets hybridkördare är unik.



EPA and EU nonroad emissions regulations: 37 – 560 kW (50 – 750 hp)



## Logset Parallel Hybrid technology



## Challenges make you stronger.

“Adding new technology adds complexity, complexity requires knowledge and new skillset in all parts of your organisation”.

Challenges and possibilities

- Component availability
- Knowledge availability
- Finding competent personnel
- Being a forerunner is also being different.
- Securing competence in aftermarket
- Technology lifespan
- Machine retail

## Logset Hybrid harvesters, possibilities ones getting things right.

” It’s an amazing machine, for the first time I’m the limiting factor, not the harvester”.  
The initial objective, to increase maximum power output, was fulfilled beyond expectation and over time we learned that the parallel hybrid technology also enabled several additional positive effects.

- The wow-effect, the feeling of limitless power and machine capacity
- Possibility to run at lower engine RPMs and maintain productivity.
- Increased productivity with reasonable fuel consumption
- Multifunctional operation without stalling the engine.
- Makes the operation of the machine more relaxed.
- Longer shifts and longer working days with higher productivity.
- Lower engine RPMs generate less vibration and less noise.
- Lower emissions, the environmental aspect
- Manufacturer image, becoming and being seen as a forerunner.

Harvester operator with 30+ years of experience

“It’s incredible, it’s a 100 cubic an hour machine”.

## Building the marketing message

“Ones understanding what the parallel hybrid technologies advantages are we also realized that we need third parties to back us up, no one would believe our statements otherwise”.

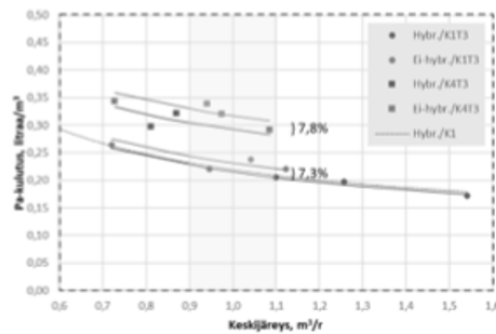
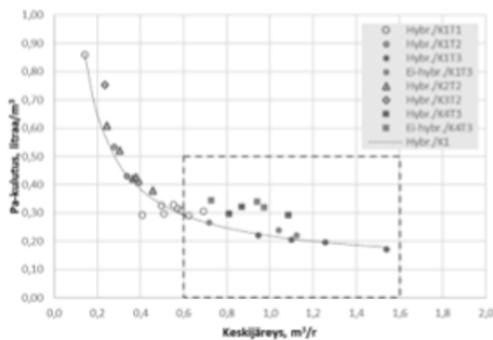


- Skogforskin Big5-testissä kesällä 2018 oli mukana viisi järeää hakkuukonetta
  - JD 1470G, Ponsse Bear, Komatsu 951, Rottne H21D, Logset 12H Hybrid
  - Testileimikkona 130-vuotias männikkö, keskijäreys 721 dm<sup>3</sup>/r (sob, kuorikorjaus 12 %)
  - Kokeneet kuljettajat
  - Kulutusta ja tuottavuutta tarkasteltiin tehoaikana (E<sub>0</sub>)



## Polttoaineen kulutus kiintokuutiota kohden keskijäreys suhteen tarkasteltuna

- Polttoaineen ominaiskulutus vaihteli selvästi sekä keskijäreys suhteen että kuljettajien välillä
- Hybridikoneen kulutus oli 7–8 % matalampi kuin hybridittömällä verkokoneella keskijäreystasolla 1 m<sup>3</sup>/r
  - Vertailuissa oletettiin, että kulutus kehittyy keskijäreys suhteen samalla tavalla kuin kuljettajan 1 hybridikoneella hakkaamissa erissä



20



# Flex-CPT hybrid powertrain concept

**Author:** Arno Amberla, *Proventia*

## Background and objective

Electrification of off-road machinery is advancing rapidly; however, internal combustion engines (ICE) will remain a core component of powertrain solutions in the foreseeable future. Key drivers include tightening emission regulations, CO<sub>2</sub> reduction targets, and the need for improved fuel efficiency and productivity.

The Flex-CPT concept focuses on system-level optimization, integrating the ICE, electric powertrain, and exhaust aftertreatment (EAT) into a balanced solution. The objective is to enhance overall performance, efficiency, and compliance rather than replace the ICE.

## Development targets and design principles

The Flex-CPT hybrid concept targets improved cost-efficiency and performance:

- Minimized CAPEX through reduced battery size and simplified architecture
- Improved durability and operational efficiency (OPEX)
- Peak shaving and smoother engine load
- Increased machine productivity and usable power output

The ICE remains the primary energy source, while the electric subsystem supports transient conditions and peak demand. Proper system sizing – especially matching motor speed and battery voltage – is critical.

## Hybrid system concept and architecture

The Flex-CPT solution is based on an ICE-dominant hybrid architecture, where the ICE provides primary energy and the electric system supports dynamic performance. This is suited for duty cycles with limited energy recovery.

The system includes an LTO battery, powertrain control unit (PECU), electric motor and inverter, and a transition from a supercapacitor-based to a battery-based solution.



**Figure 1.** Hybrid system architecture at test laboratory



### Performance characteristics and test results

Hybridization significantly improves dynamic performance: diesel torque response is ~3 seconds at low rpm, electric response ~1 second, and combined system reaches ~85% torque in less than 1 second.

The hybrid increases available power from a 214-kW base engine to approximately 320–350 kW.

No direct fuel consumption reduction was observed due to lack of energy recovery. However, improved transient response and higher power enable significantly higher productivity in the target application, increasing operational throughput.

### System integration: EAT, thermal and safety

Hybridization stabilizes exhaust temperatures, reducing the need for active thermal management. Higher power increases thermal loads, requiring insulation. Safety features include high-voltage compliance and limp-home functionality. Optimized component matching can reduce system complexity and cost.

The Flex-CPT hybrid enables higher power density, faster transient response, and increased productivity. The main benefit is improved system performance rather than direct fuel savings. In suitable applications, this results in significantly higher effective output and operational efficiency.

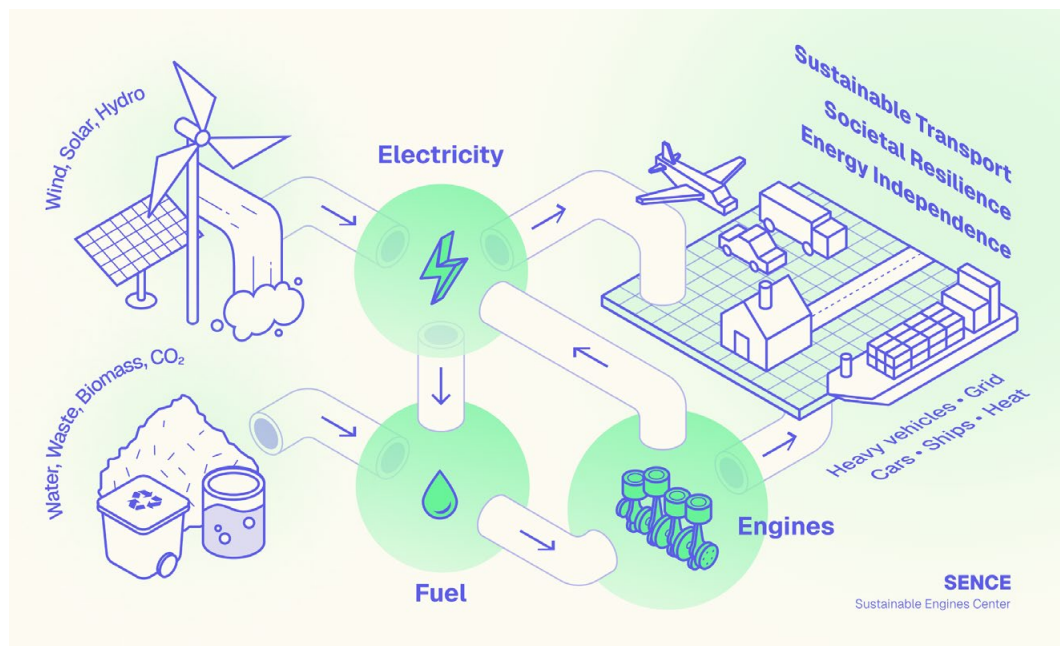


# Lessons from Road Vehicle Powertrains for The Future Sustainable Off-Road Applications

**Author:** Martin Tunér, *Lund University, Sweden*

The use of fossil fuels has built the modern world, but has reached levels that are not sustainable. The consequences can be summarized in emissions of greenhouse gas emissions that lead to climate damage, but also in wars over oil and the prevention of democratic development. The cost of these are estimated to 55 trillion USD annually while the cost to mitigate these would only account to one tenth, 5.5 trillion USD annually.

The scale of the global challenge to reduce the use of fossil fuels is gigantic and there is no option but to use several complementing resources like solar, wind, hydro, biomass, waste and captured CO<sub>2</sub>, and several technologies that operate in parallel, such as electric drive, combustion engines and gas turbines.

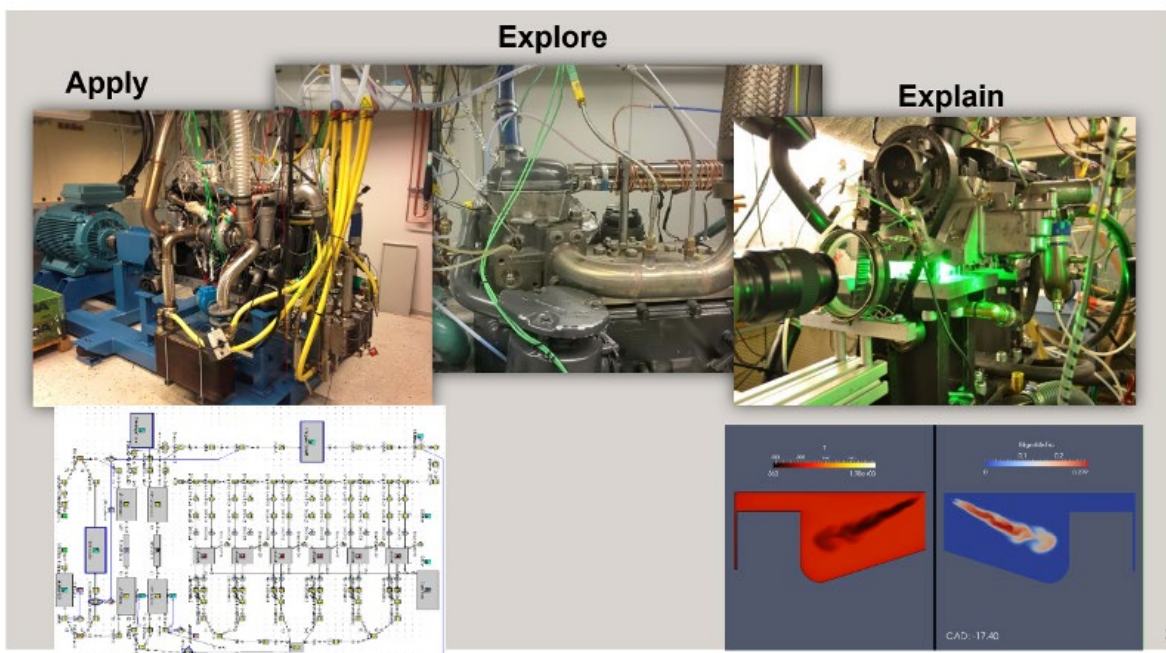


Several non-commercial organizations predict that engines will play an important role far into the future in complementing electrification for sustainable energy generation and for motive systems. The Intergovernmental Panel on Climate Change (IPCC) says that fuel efficient vehicles and ships are the fastest and most cost-efficient options to mitigate climate damage, while biofuels, electrofuels and electric & hybrid electric vehicles are other important measures.

The role of academic research is therefore to investigate how engines can be made more efficient while being adapted to new sustainable fuels. The academics focus on exploring and explaining the fundamentals while the collaboration and information sharing with the automotive industry means that real world problems are researched and that results from research can reach market faster.

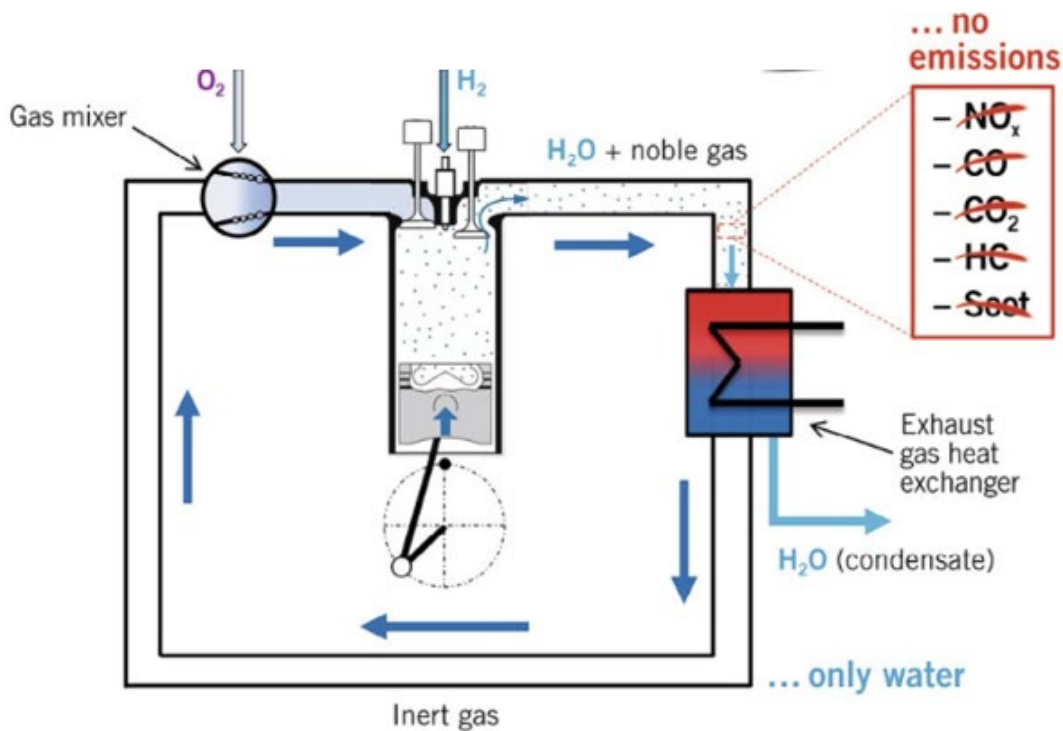
The research at Lund University has demonstrated how engines can be true omnivores and operate on a number of different energy resources such as HVO, ethanol, methanol, hydrogen, biogas and other. The use of developed advanced diagnostic techniques help to understand the combustion of various fuels and provide insights that are used to develop tools that help the development of sustainable engines for road and off-road applications.

The presentation contains a wealth of information regarding the characteristics and performance of different fuels when combined with novel advanced combustion strategies. The combination of experimental and numerical research works hand-in-hand to address different types of questions providing overall enhanced quality of the research. The combination provide both scientific depth and breadth ultimately leading to trained experts for the benefit of society and for our partner companies.



The results show that each fuel comes with its own set of opportunities and challenges. Hydrogen can provide higher efficiency than conventional fossil fuels like diesel or gasoline, while at the same time avoid CO, CO<sub>2</sub> and soot emissions altogether. Injection and in-cylinder mixing as well as onboard handling of hydrogen gas are some of the challenges that are being researched. Alcohols have the benefit of being liquids and do also lend them selves to high efficiency operation with strongly reduced emissions. Cold starting and corrosion are examples of areas under research in this case. Biogas can in the broader picture even provide negative green-house gas emissions. How to increase efficiency and minimize methane slip is some topics being researched here.

The advanced combustion concepts such as HCCI and PPC has provided deeper insights of the combustion phenomena and offers a wide range of tools for clean and efficient engine operation. More recently engines without tailpipe, and therefore no emissions, are being researched. The idea is to operate with a closed cycle using a noble gas as working media. Combined with hydrogen and oxygen the only byproduct is water. Research show that there is also potential for very high efficiency, but considering the many interesting challenges of the concept, we can conclude that the jury is currently still out.



# Policy Measures to Accelerate the Decarbonisation of Non-Road Mobile Machinery

**Author:** Kaarina Kaminen, *Finnish Environment Institute*

## Greenhouse gas emissions from non-road mobile machinery

Greenhouse gas emissions from non-road mobile machinery (NRMM) have remained stable during the last decades although the local emissions have declined. In 2023, emissions from NRMM amounted to approximately 2,4 Mt CO<sub>2e</sub>, representing roughly 5% of Finland's total greenhouse gas emissions (excluding LULUCF emissions) (Ministry of the Environment, 2025). According to stakeholders' views, a major challenge is the lack of strong and predictable policy instruments. The availability of zero-emission and low-emission machinery is still limited, while high investment costs hinder the adoption of new technologies. However, the adoption of alternative propulsion systems is already partly market-driven (Karhinen et al., 2026).

## Current and upcoming policy measures

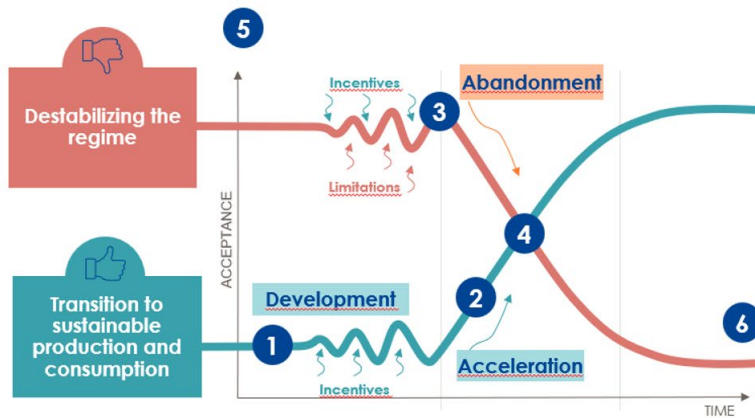
The regulatory framework to decarbonize mobile machinery is relatively undeveloped in Finland as well as in the European Union. The distribution obligation for biofuel oil has been one of the main national policy measures to support greenhouse gas emission reductions from NRMM, requiring fuel distributors to increase the share of biofuels (to 8% in 2026) supplied to the market. In addition, taxes on liquid fuels and electricity affect the profitability of investments in alternative powertrains as well as in charging and distribution infrastructure. Light fuel oil has been subject to a substantial tax subsidy. The emissions trading scheme for road transport, buildings and other sectors (ETS2), a major new policy tool, will be launched in 2028, raising petrol and diesel prices by 7–14% by 2030 according to the estimates of the European Commission. In contrast to the transport sector, there have been no procurement subsidies to support the transition to clean technologies. The voluntary agreements, the green deals, have increased the demand for and supply of alternative propulsion systems. RDI funding has been allocated to the development of alternative powertrains in NRMM, and public RDI funding is expected to increase both nationally and in the European Union's Multiannual Financial Framework (MFF) for 2028–2034.

## Policy interventions to accelerate the sustainability transition

The sustainability transition requires an effective policy mix that stimulates the creation and diffusion of sustainable innovations, phases out unsustainable practices, supports vulnerable groups affected by the transition, and enhances coordination and the setting of binding targets (e.g. Kanger et al., 2020). The theoretical framework suggests that policy interventions in the NRMM sector should be reinforced across all these dimensions. According to our analysis (Auvinen et al., 2025), policy measures should be designed to accelerate the use of alternative powertrains especially in industrial areas where machinery use is intensive. Charging and energy infrastructure should be developed to serve both machinery and heavy-duty vehicles, thereby maximizing cost-effectiveness.



## X curve: Policy interventions for the sustainability transition



- 1. Encouraging the creation of innovations:** RDI funding, tax deductions for RDI activities, experiments, innovation incubators
- 2. Supporting the diffusion of innovations:** Investment subsidies, financial programmes, financial incentives, advice, communication, standards, labelling, public procurement
- 3. Abandoning unsustainable practices and technologies:** Phasing out harmful subsidies, emissions trading, carbon taxes, technology ban
- 4. Addressing the adverse effects of the transition:** Retraining, skills needs mapping, employment programmes, social benefits, compensations, transition periods
- 5. Cross-sectoral cooperation:** Cross-sectoral strategies, impact assessments, emission calculation
- 6. Setting binding targets:** Long-term targets, roadmaps

Source: Kanger et al. (2020), <https://doi.org/10.1016/j.respol.2020.104072>



# Technical Sessions



# NVO Fuel Injection for Low-Load Extension of RCCI

**Authors:** Amir Soleimani, Jeyoung Kim, Jacek Hunicz

**Keywords:** RCCI; negative valve overlap; NVO fuel injection; low-load extension; combustion stability; methane emissions; variable valve actuation

## Background and objective

Marine propulsion is moving toward lower greenhouse-gas emissions, higher efficiency, lower NO<sub>x</sub>/PM, and wider fuel flexibility. RCCI is a promising combustion concept for this transition because it can combine high efficiency, low soot/PM, lower NO<sub>x</sub>, and flexible fuel use. However, unlike conventional diesel combustion, RCCI autoignition is governed by the thermal and chemical reactivity of the mixture, which makes combustion control more complex.

At very low load, this limitation becomes more critical. Low charge reactivity can reduce combustion efficiency, increase cyclic instability, and increase methane slip in NG–diesel RCCI operation. Therefore, this presentation examined NVO diesel injection as a possible strategy for RCCI low-load extension by using recompression-period fuel injection to support the following main combustion event.

## Approach

The work was performed on the University of Vaasa W4L20 research engine platform, with one RCCI cylinder and three conventional diesel cylinders. The RCCI cylinder is used for this experiment and is equipped with fully electro-hydraulic valve actuation, enabling flexible control of valve timing and NVO operation. Emissions were measured using FTIR, and data acquisition was carried out using Dewesoft.

The investigated combustion mode was NG–diesel RCCI at 1000 rpm and very low load. A symmetric 100°CA NVO window was used. The main variables were NVO diesel start of injection and NVO diesel energy fraction. The analysis focused on combustion phasing, stability, NVO heat release, load response, and emissions.

## Key results

The timing sweep first showed that NVO diesel injection influenced the following main combustion event only when the injection was placed near NVO TDC. As shown in Fig. 1, SOI around 360°CA bTDC produced a clear response: CA<sub>50</sub> advanced and the COV of IMEP dropped below the 5% stability threshold, indicating stabilization of an otherwise unstable very-low-load RCCI point. When the injection was shifted later, this effect was no longer clearly observed. CA<sub>50</sub> changed only slightly, suggesting that the NVO-injected fuel mainly acted as a broadly mixed contribution to the next cycle rather than providing a distinct combustion-control effect.

The CHR traces in Figure. 1 show the origin of this timing-dependent response. Only the near-TDC injection produced clear apparent heat release during the NVO period, indicating that the useful mechanism was mainly thermal. When injection was properly phased, part of the fuel energy was released during recompression and helped support the following main combustion event; for later timings, this thermal contribution was largely absent.

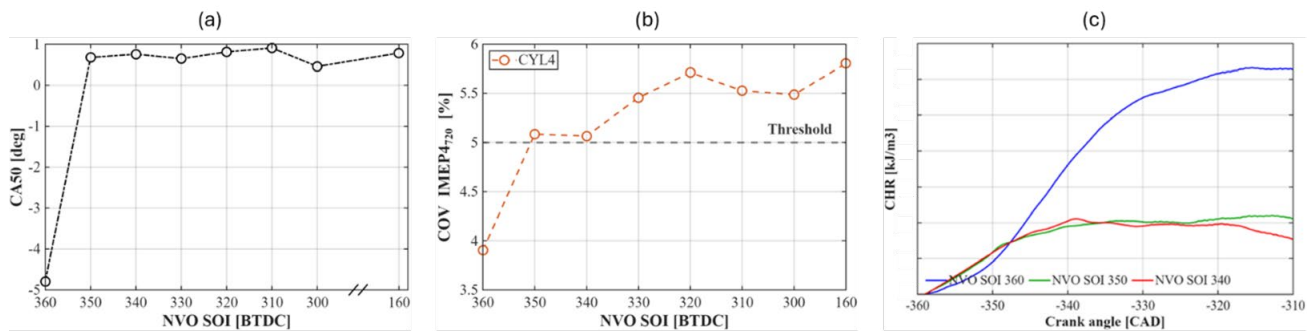


**Figure 1.** NVO injection timing sweep at fixed NVO energy fraction: (a) CA50 as a function of NVO SOI; (b) COV of IMEP as a function of NVO SOI, with the 5% stability threshold; (c) cumulative heat release during the NVO interval for selected NVO SOI timings.

The split-ratio results in Figure. 2 then show how this mechanism changes when more diesel is shifted from the main injection to the NVO injection. Near 360°CA bTDC, increasing the NVO fuel fraction strengthened the apparent NVO heat release, advanced combustion phasing, and improved stability. However, the same trend also reduced net indicated load, because part of the fuel energy was released before the main combustion event and the combustion phasing became over-advanced.

Away from the effective NVO-TDC timing window, increasing the NVO split became detrimental. Since the thermal benefit was weak, the dominant effect was the reduced diesel share in the main injection event. This weakened reactivity stratification, delayed combustion, and increased instability at higher split ratios. The emissions response followed the same combustion behaviour: near 360°CA bTDC, higher NVO ratios increased NO<sub>x</sub> due to advanced phasing, whereas ineffective timings increased CH<sub>4</sub>, CO, and NMHC because of poorer combustion efficiency.

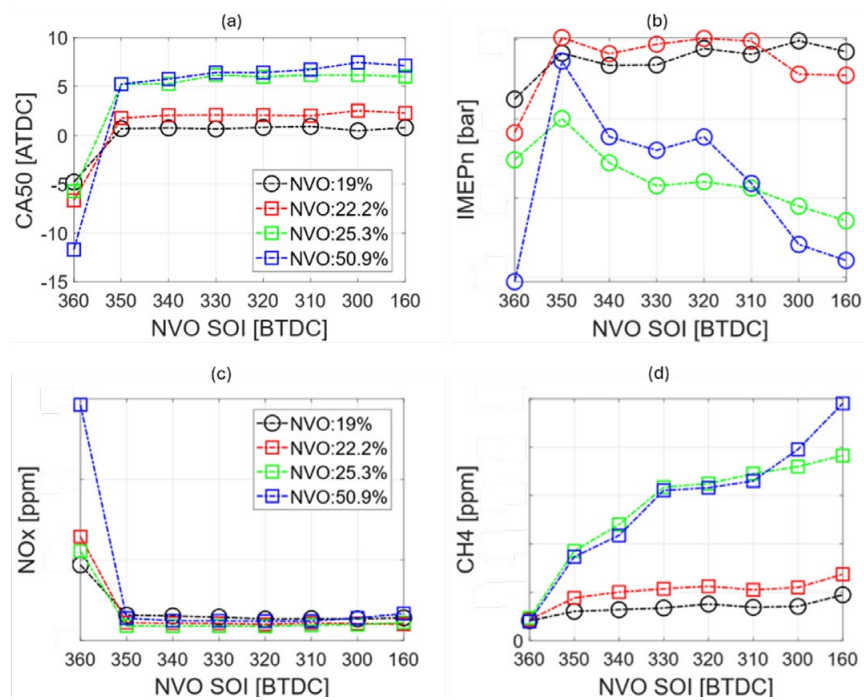


**Figure 2.** NVO injection timing and split-ratio sweep: (a) CA50 as a function of NVO SOI for different NVO energy fractions; (b) net indicated mean effective pressure as a function of NVO SOI; (c) NO<sub>x</sub> emissions as a function of NVO SOI; (d) CH<sub>4</sub> emissions as a function of NVO SOI



# Adaptive Modelling & On-Board Optimal Control of RCCI Combustion

**Authors:** Amir Talebi Sheikhsarmast, Mohammad Raisi Esfarjani, Amir-Mohammad Shamekhi, Xiaoguo Storm, Amin Modabberian, Jeremias Pohjola, Arto Visala, Maciej Mikulski

**Keywords:** RCCI combustion, extremum seeking optimization, data-driven RCCI modelling, adaptive MPC, fuel-flexible control

This presentation summarized recent progress on adaptive optimization and data-driven modelling of marine RCCI combustion within the Flex-CPT project. The work supports future clean propulsion through real-time optimization and predictive combustion control for low-emission marine engines. Since RCCI combustion is highly nonlinear and strongly dependent on operating conditions, the study focuses on advanced control of Start of Injection (SOI), Blend Ratio (BR), and total fuel energy to regulate combustion phasing (CA50) and engine performance (IMEP). The first technical part presented an adaptive real-time Extremum Seeking (ES) optimization framework implemented on the Wärtsilä W4L20 RCCI engine. The developed optimizer enables real-time co-optimization between ultra-low NO<sub>x</sub> emissions and stable RCCI combustion under varying operating conditions. Experimental validation demonstrated stable low-emission RCCI operation across multiple operating conditions. In addition, the ES framework was used to construct an experimentally validated optimal CA50 reference map, which forms the foundation for future closed-loop RCCI combustion control. The accepted paper will be presented at IFAC World Congress 2026.

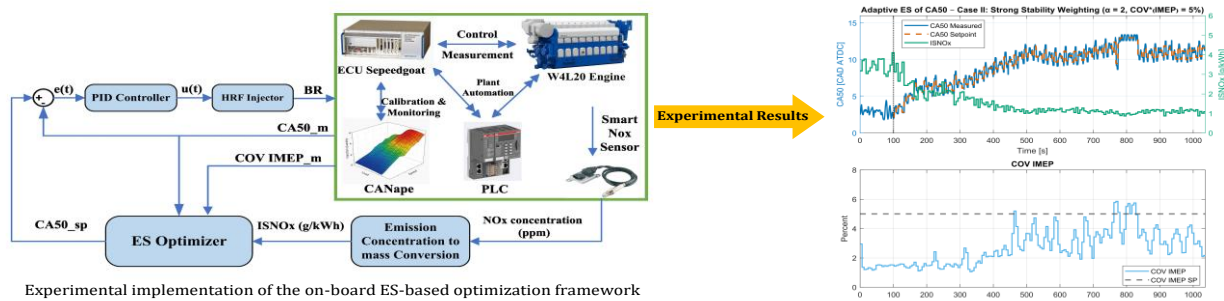
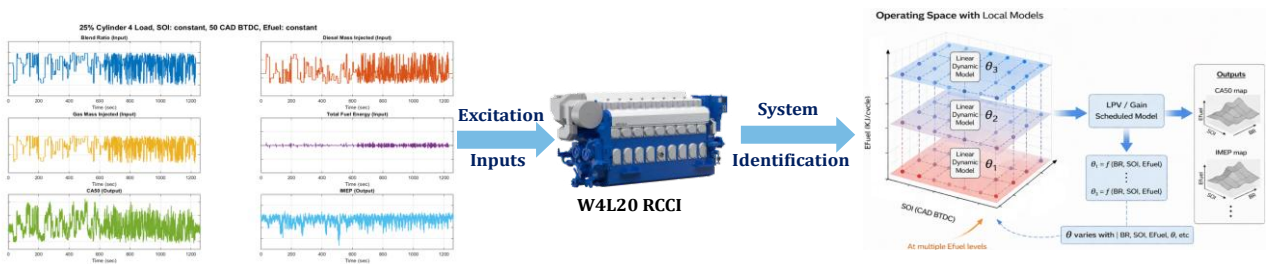


**Figure 1.** Experiment implementation of the on-board ES-based optimization framework.

The second part focused on high-fidelity LPV data-driven modelling of RCCI combustion dynamics for real-time control applications. Extensive multi-load experimental campaigns were conducted by systematically exciting SOI, BR, and fuel energy inputs independently and simultaneously. The generated datasets enabled system identification of highly accurate linear dynamic models capable of real-time prediction of CA50 and IMEP. Compared to computationally expensive physics-based RCCI models, the proposed LPV framework provides a computationally efficient and control-oriented representation suitable for future adaptive MIMO MPC combustion control. Overall, the results demonstrate strong potential of combining adaptive optimization and high-fidelity data-driven modelling for robust and real-time RCCI control in next-generation fuel-flexible propulsion systems.



Advanced Experimental Campaign for Data-Driven RCCI Modeling

Figure 2. Advanced experiment campaign for data-driven RCCI modelling

The final part presents an adaptive Model Predictive Control (MPC) framework combined with online Recursive Least Squares (RLS) for real-time RCCI combustion control. Due to the strong nonlinearity and operating-condition dependence of RCCI, fixed models and conventional controllers are insufficient, motivating the use of adaptive and data-driven strategies.

The proposed framework integrates online system identification and control in a closed-loop structure, where an ARX model is continuously updated via RLS using real-time CA50 and IMEP measurements. The updated model is then used by the MPC to compute optimal control inputs while handling multivariable interactions and operational constraints. The approach provides a computationally efficient and practical solution suitable for real-time implementation.

The methodology is validated using both the UVATZ multi-zone physics-based model and the nonlinear control-oriented COM model. Compared to a decentralized PI controller, the adaptive MPC achieves improved tracking performance, reduced errors for CA50 and IMEP, and smoother control inputs. While the PI controller exhibits faster transient response, it shows larger deviations and weaker handling of coupled dynamics, confirming the advantage of the adaptive approach.

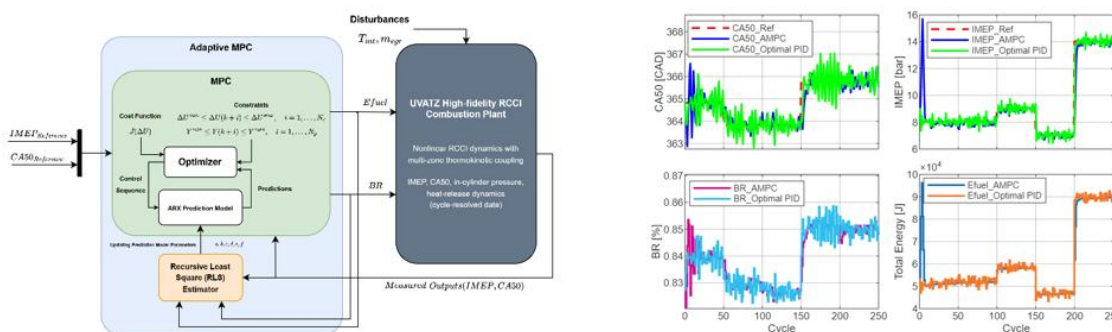


Figure 3. Adaptive MPC structure and performance comparison.

The framework is further implemented and validated on the Wärtsilä W4L20 RCCI engine over a load range of 0–50%. Standard identification tests, including residual whiteness, regressor independence, and parameter convergence, confirm stable and reliable online estimation. The resulting ARX-RLS model achieves prediction accuracy of approximately 87% for CA50 and 91% for IMEP, demonstrating strong capability for real-time combustion prediction.

Overall, the results show that adaptive MPC with online RLS provides a robust, accurate, and implementation-ready solution for RCCI combustion control, enabling improved performance and supporting real-time deployment.

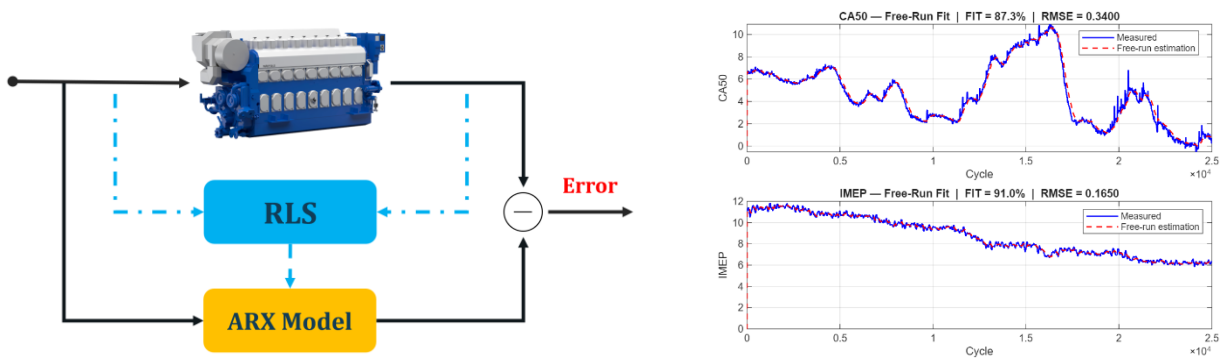


Figure 4. ARX-RLS model validation on W4L20 engine.

# Hydrogen Engine Blow-by: Modelling, Validation, and Design Insight

**Author:** Touraj Hashempour

**Keywords:** Hydrogen engine; blow-by; ring pack; 1D simulation; GT-Power

## Motivation and objective

Hydrogen internal combustion engines require reliable blow-by prediction because hydrogen-containing leakage through the piston ring pack can increase crankcase flammability risk, affect lubricant durability, and determine the required ventilation capacity. The presentation focused on a physics-based 1D approach for predicting hydrogen engine blow-by, identifying dominant deviation sources, and translating the model results into design guidance for ring pack development and crankcase ventilation sizing.

## Modelling framework and experimental comparison

A GT-Power ring pack and cylinder model was used to represent the principal leakage routes: ring end gap leakage, flow around the ring in the groove, and leakage between the ring face and cylinder wall. The model was directly coupled to calibrated cylinder pressure boundary conditions obtained from measured engine data. The crankcase side was represented as a control volume vented to ambient, and species mass flow tracking was added to evaluate both total blow-by and hydrogen-containing blow-by consistently.

The framework was compared against measured data from a hydrogen engine test campaign. Three Pressure Analysis was used to derive operating point specific burn rate data and reproduce the measured in-cylinder pressure boundary. The validation basis included blow-by gas mass flow and hydrogen concentration. The operating range included low/high speed and low/high load conditions, which made it possible to assess both trend prediction and operating point-specific deviations.

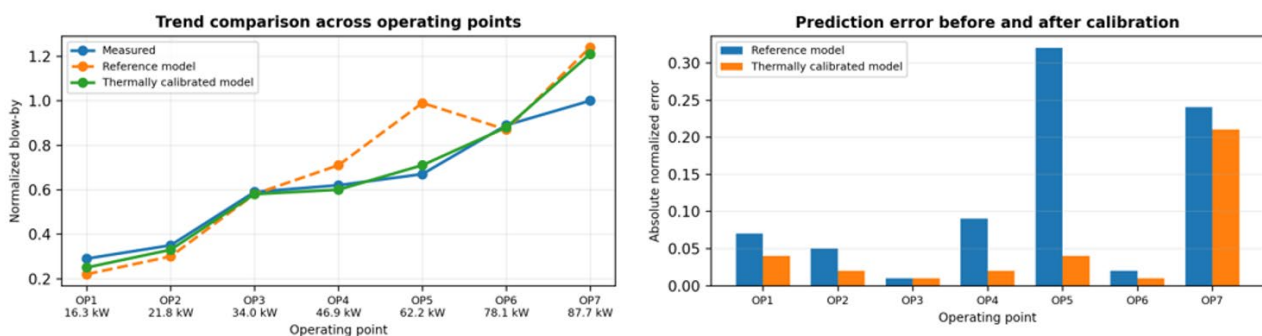


**Figure 1.** Normalized blow-by trend and absolute prediction error before and after thermal calibration.

## Key results and outcomes

- The reference model captured the overall measured blow-by trend, but large deviations appeared at specific operating points where the effective ring thermal state strongly affected the hot ring end gap.
- The main model for measurement deviation was linked to temperature-dependent ring behaviour: higher ring temperature reduces the effective end gap and therefore lowers predicted leakage through the ring pack throttling path.
- After thermal calibration, agreement improved substantially: mean absolute error decreased from 1.43 to 0.65, root mean square error from 1.99 to 1.04, mean absolute percentage error from 18% to 8%, and correlation increased from 0.57 to 0.88.
- The parametric study showed that the designed ring end gap was the dominant sensitivity parameter. A +20% end gap perturbation increased predicted blow-by by 28.5%, while a -20% perturbation reduced it by 34.0%.
- Over the selected practical perturbation ranges, end gap produced the largest average design impact (31.2%), followed by axial thickness (5.7%), ring tension (4.5%), and ring mass (0.5%).

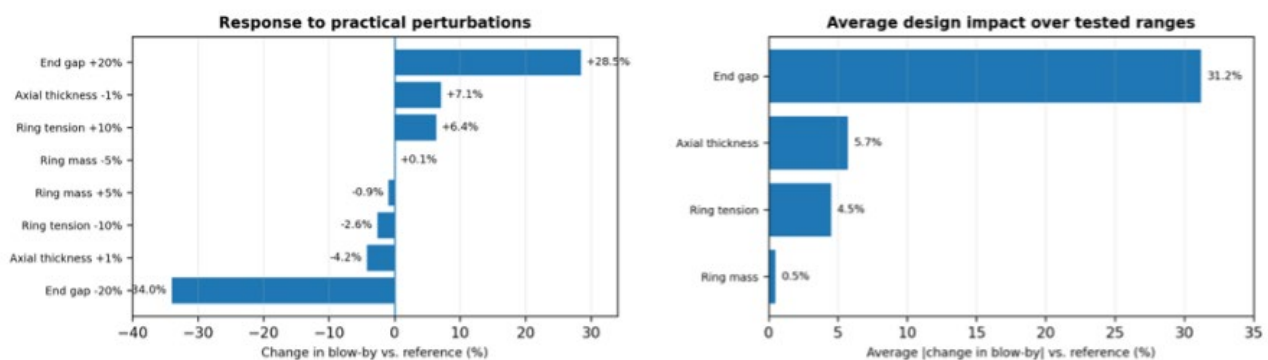


**Figure 2.** Ring pack design sensitivity: response to individual perturbations and average design impact.

## Engineering value and next steps

The work demonstrates that a calibrated 1D ring pack model can be used as a design-oriented tool for early assessment of hydrogen blow-by risk. The model links measured and calibrated cylinder pressure behaviour to ring pack leakage, identifies temperature-sensitive sealing mechanisms, and supports design decisions related to end gap selection, ring package refinement, and crankcase ventilation requirements.

The next development steps are to extend the approach from a single cylinder configuration to multi-cylinder system level prediction, replace empirical thermal calibration with predictive ring thermal modelling, and couple the blow-by model with a crankcase ventilation model. This integration will support purge flow sizing, ventilation architecture evaluation, and safer hydrogen engine crankcase design. The results also support the planned publication on integrated 1D ring pack and cylinder modelling and validation for hydrogen engine blow-by investigation.

# Towards Heavy Duty Spark Ignited Methanol Engines

**Authors:** Mayanka Jha, Olli Ranta, Joakim Kapp, Qiang Cheng, Otto Blomstedt, Ossi Kaario

**Keywords:** Spark ignited engine, methanol combustion, port fuel injection, combustion analysis, OH\* chemiluminescence.

## Introduction and objective

The presentation focused on describing the early stage of methanol combustion experiments in the research engines of Aalto University. With the motivation to study the effect of premixed methanol as an alternative fuel in a spark ignition heavy-duty engine, the investigation was conducted in both full metal research engine as well as the optical engine. By combining the investigation on both the engines, it was possible to follow the cold-start problems, often encountered with alcohol fuel such as methanol.

## Methodology

Following a systematic approach, the experiments were conducted in full-metal engine at a particular engine speed of 1000 RPM, in a naturally aspirated mode. At this fixed engine speed, three parameters were swept: intake air temperature,  $\lambda$  and spark ignition timing. Additionally, in order to reduce the cold start duration, the engine operations were always initiated with rich conditions ( $\lambda \sim 0,7$ ) and advanced spark timings (16/18 DBTDC). Furthermore, due to the absence of lambda control, the  $\lambda$  values were fixed at approximately and not exactly the targetted values. This was achieved by manually altering the injection duration on the basis of lambda sensor values.

The full-metal engine results indicated that an early combustion phasing and shorter duration can be achieved with higher intake air temperature (at constant  $\lambda$  and fixed spark timing), richer conditions (at fixed intake air temperature and spark timing) or early spark timing (at constant  $\lambda$  and intake air temperature). Additionally, the measured fast measurement data revealed that both cylinder pressure and heat release rate (HRR) decrease with lower intake air temperature, leaner conditions ( $\lambda > 1$ ) and later spark timing. Figure 1 presents the HRR and cylinder pressure curves for the test case where  $\lambda$  was varied while maintaining an intake air heater temperature of 120°C and a spark timing 16 DBTDC.

However, through endoscopic visualisation into the intake runner, it was confirmed that not all of the liquid methanol was getting evaporated. This situation was observed, despite a recorded drop in the intake air temperature after the methanol injectors. Therefore, it was concluded that heating up only the intake air (especially to the levels used in this investigation) was not enough to ensure complete vaporization of the injected methanol. Additionally, such an approach of heating up the intake air also caused some changes in target  $\lambda$  values.

The experiments were further extended in the optical engine as well, where premixed methanol spark ignited, combustion was visualised using OH\* chemiluminescence imaging technique at an engine speed of 1000 RPM. Unlike full-metal engine, optical engine was operated in skip-firing mode, such that there were 9 consecutive fired cycles followed by 50 consecutive unfired/skip-fired cycles. This sequence was repeated 7 times, with the camera recording every 7<sup>th</sup> fired cycles (therefore capturing a total of 7 cycles, from a total of 63 fired cycles).

After multiple parameter iterations (compression ratio, spark dwell time, spark ignition timing, intake air temperature and  $\lambda$ ), it was finally possible to find a combination of operational parameters, which would produce cycles with methanol combustion and visualisation of flames with strong OH\* signals.

Following the combination, the optical engine was run at a constant engine speed of 1000 RPM,  $\lambda = 0,5$ , compression ratio  $\sim 15$  and intake air temperature  $\sim 70-75^\circ\text{C}$ . Additionally, in these runs only the spark ignition timing was varied at 15 and 10 DBTDC.

The test sweeps in the optical engine revealed that with an advanced spark timing of 15 DBTDC, there were couple of cycles where autoignition was visible, however there were no signs of knocking cycles. With later spark timing of 10 DBTDC, there was just one cycle with autoignition (no knocking recorded). Therefore, it was concluded that the optimal spark timing may be between 10 and 15 DBTDC. Nevertheless, the optical results were in agreement with the full-metal engine results, such that a decrease in cylinder pressure was observed with later spark timing. Figure 2, presents the cycle-to-cycle variation of OH\* chemiluminescence signal, when spark timing of 15 DBTDC was maintained.

## Conclusions

In conclusion, a key limitation identified through these initial test runs with were the incomplete evaporation of the liquid fuel, and lambda fluctuations. Therefore, for future runs, the engine is planned to be operated with lambda control to eliminate lambda fluctuations. Furthermore, discussions to improve vaporization of methanol with other alternative methods (such as fuel heating) has also been started.

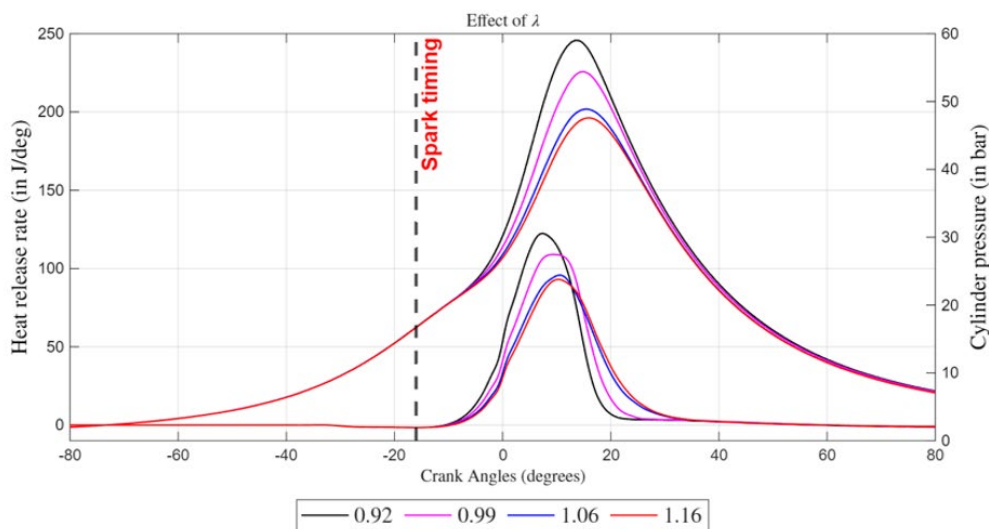


**Figure 1.** HRR (left axis) and cylinder pressure (right axis) trends as a function of crank angles for various  $\lambda$  at a constant intake air temperature and spark timing.

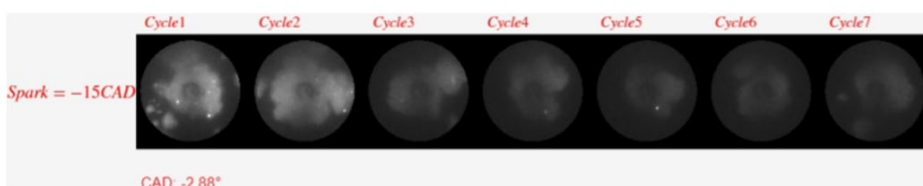


**Figure 2.** Cyclic variation of OH\* chemiluminescence signal at 15 DBTDC of spark timing.

# An environmental and Economic Assessment of a Medium-sized Wheel Loader: a Nordic Case Study

**Authors:** Anthony Katumwesigye, Jonas Spohr, Magnus Hellström, Reyn O´Born

**Keywords:** Non-road mobile machinery, electrification, hydrogen, life cycle assessment (LCA), techno-economic analysis (TEA), decarbonisation, Nordic energy systems

## Introduction and objective

The study conducted addresses the growing challenge of decarbonising non-road mobile machinery (NRMM), a sector that is particularly difficult to transform due to its high-power requirements, extended duty cycles, and operational constraints. Conventional approaches focusing solely on tailpipe emissions are insufficient, as they overlook upstream emissions and infrastructure dependencies.

Within this context, the study examines a medium-sized wheel loader operating under Nordic quarry conditions, with the aim of identifying the most effective propulsion pathway among diesel internal combustion engines (ICE), battery-electric vehicles (BEV), and hydrogen fuel-cell electric vehicles (FCEV). The objective is to determine under what conditions each pathway achieves environmental and economic competitiveness when evaluated on a consistent work basis.

## Methodology

The study applies an integrated framework combining life cycle assessment (LCA) and techno-economic analysis (TEA), ensuring that both environmental and economic metrics are aligned to a shared functional unit defined by tonnes of material moved. Three propulsion pathways—diesel, battery-electric, and hydrogen fuel-cell—are analysed within a unified system boundary covering machinery production, energy supply, infrastructure, and operation.

The analysis accounts for four Nordic electricity contexts (Finland, Sweden, Norway, and Denmark), capturing differences in grid carbon intensity, energy prices, and policy environments. Infrastructure is explicitly modelled, including charging systems for BEVs and hydrogen supply chains for FCEVs.

Uncertainty is addressed through Monte Carlo simulation, incorporating variation in costs, productivity, and energy prices. This enables a robust comparison not only of average results but also associated risks.

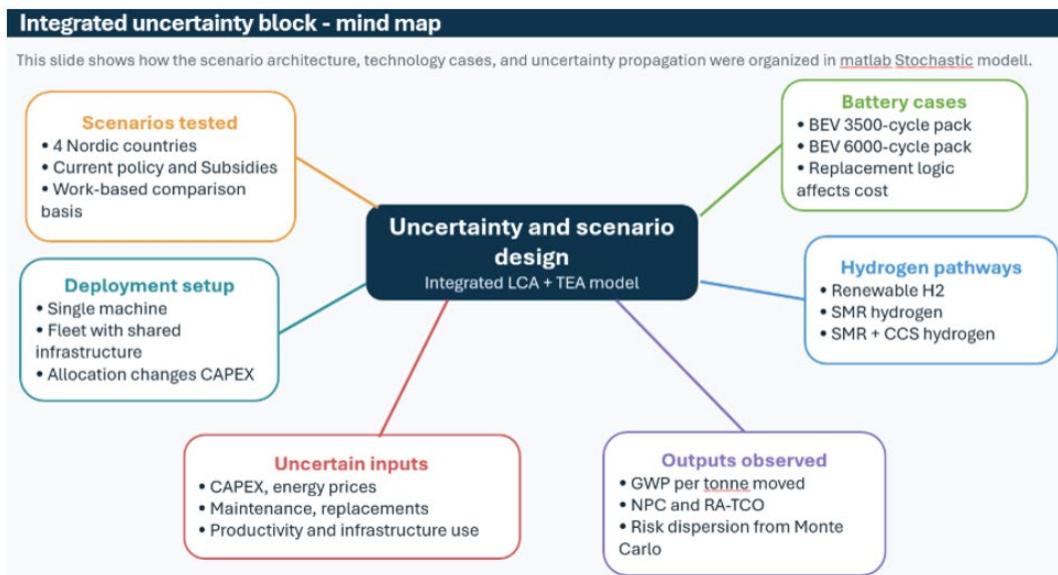


**Figure 1.** Set up of Uncertainty Block in MATLAB.

## Results and discussion

The environmental results show that battery-electric systems achieve substantially lower emissions than diesel, with values ranging from approximately 0.04–0.13 kg CO<sub>2</sub>-eq per tonne moved, compared to roughly 1.13 kg CO<sub>2</sub>-eq for diesel. Hydrogen systems show highly variable results depending on production pathways, with low-carbon hydrogen performing well but carbon-intensive pathways potentially exceeding diesel emissions.

Electricity carbon intensity plays a decisive role, as differences across Nordic grids significantly influence results, especially for hydrogen pathways. The study highlights that electrification shifts environmental burdens to the manufacturing stage, where batteries and fuel-cell systems contribute significantly to emissions.

From an economic perspective, battery-electric systems are the most competitive, with costs ranging between 0.27–0.32 €/t moved, compared to 0.41 €/t for diesel and 0.67–0.91 €/t for hydrogen. Policy measures primarily support electrification, while hydrogen remains constrained by high fuel costs.

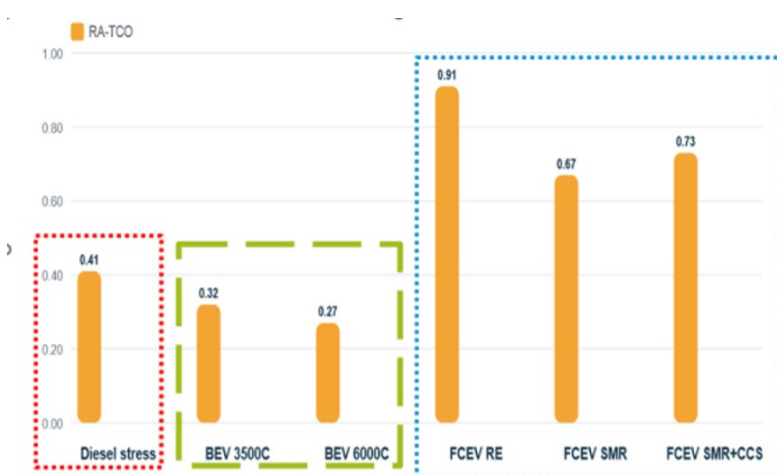


**Figure 2.** Economic performance of studied NRMM propulsion technologies



## **Conclusions**

The study concludes that battery-electric propulsion represents the most robust decarbonisation pathway for medium-sized wheel loaders in Nordic conditions. Hydrogen remains context-dependent and requires significant cost and policy support to become competitive.

Overall, the findings emphasise that decarbonisation outcomes are shaped by the interaction between technology, energy systems, infrastructure, and policy. A full life-cycle perspective is essential to ensure accurate evaluation and effective decision-making in the transition of non-road mobile machinery.



# Comparative Well-to-Wake GHG Performance of Alternative Marine Fuels in Cruise Shipping Across LCA Frameworks

**Authors:** Ramtin Heydarian, Magnus Hellström, Anastasia Tsvetkova, Jonas Spohr

**Keywords:** Life Cycle assessment; maritime decarbonization; cruise industry; compliance costs; IMO and RED II LCA guidelines; alternative fuels

## Introduction

Comparative WtW Life Cycle Assessment of 9 maritime alternative fuels is implemented (MeOH<sup>3</sup>, LNG<sup>3</sup>, HVO<sup>2</sup>, EtOH<sup>3</sup>) according to Renewable Energy Directive (RED II), International Maritime Organization (IMO) LCA guidelines, and IMO default values.

## Goal & Scope

- ✓ Environmental performance per MJ alternative fuel, incorporating:
  - IPCC AR5 GWP, Energy-based allocation
  - Operational modes (transit, manoeuvring, berth)
  - Engine load variability, corresponding efficiency, methane slip.
- ✓ Comparison of LCA regulatory choices (IMO vs RED, emission factors vs modelling)
- ✓ Integrating fuel costs for different alternative fuels with regulatory compliance cost under the FuelEU Maritime regulation and the EU ETS

## Findings

Methanol (MeOH) demonstrated a comparatively higher potential for decarbonization followed by renewable diesel. Ethanol (EtOH) production is highly energy intensive. Although feedstock (Sugarcane bagasse) is assumed as a waste, the environmental performance still appears suboptimal. The choice of assessment framework (IMO vs. RED) can lead to notable differences in Well-to-Wake (WtW).



Mediterranean Scenarios	RED II	IMO default values	IMO calculated values	Unit
Bio-methanol	4.18	4.18	4.18	g CO <sub>2</sub> /MJ
Bio-e-methanol	8.02	8.02	8.02	g CO <sub>2</sub> /MJ
E-methanol (DAC)	10.64	10.64	10.64	g CO <sub>2</sub> /MJ
Bio-methane	34.3	39.3	26.6	g CO <sub>2</sub> /MJ
E-methane (flue gas)	35.03	40	27.38	g CO <sub>2</sub> /MJ
E-methane (DAC)	34.1	39.1	26.4	g CO <sub>2</sub> /MJ
Renewable diesel-1	8.47	9.58	-	g CO <sub>2</sub> /MJ
Renewable diesel-2	12.26	13.4	-	g CO <sub>2</sub> /MJ
Bio-ethanol	39.73	39.73	39.73	g CO <sub>2</sub> /MJ

**Table 1.** Net WtW results for Mediterranean (M) and Caribbean routes (C1 & C2), based on RED II (SimaPro), IMO calculated figures using combustion profiles (IC), and IMO default values (ID), under IPCC-consistent biogenic CO<sub>2</sub>

IMO default values failed to reflect operational modes and currently obtains limited impact as kept on hold. RED II provides better formulation for emission calculations, especially when using LCA software. Methanol and HVO showed greater economic potential in the long term, whereas methane will cost roughly twice the same energy demand (due to compliance cost). VLSFO will cost more than alternative fuels, from 2040 onwards. Electro-fuels will cost comparable to bio-fuels in the long term.

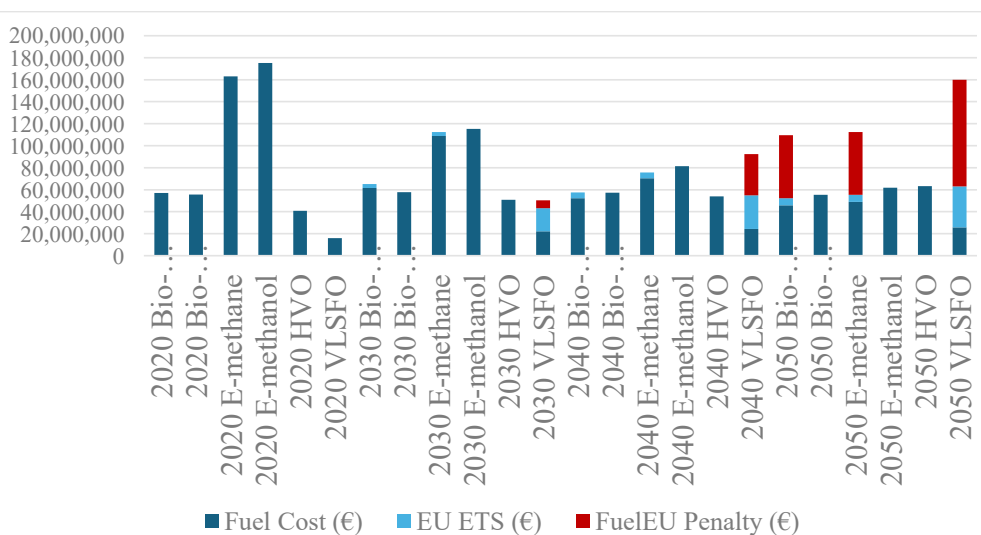


**Figure 1.** Integrated cost assessment of alternative fuels including compliance cost derived from FUELEU and EU ETS.



# Large-Eddy Simulations of Droplet Size Effects in Early - Stage Urea-Water Spray Injection

**Authors:** Haneef Azher, Shervin Karimkashiarani, Ville Vuorinen, Lasse Tuominen, Aki Kärnä, Viktor Heir Anders

**Keywords:** Urea-Water solution (uws) sprays, droplet size effects, large-eddy simulation (LES), multi-component evaporation, preferential concentration

## Summary

The research was done to address the research gap in understanding the behaviours of low-pressure injection industrial Urea-Water Solution sprays, initialized with varying droplet sizes. The flow of the presentation was as follows,

- First, a comparison of an industrial Urea-Water Spray was done with an industrial Diesel spray, to convey a preliminary understanding of the characteristics of the Urea-water spray.
- Second, the details of the case setup for the numerical simulations were given.
- Then, verification of the numerical model was shown through a grid-independence study.
- Following this, results of a 0D multi-component evaporation model were shown to understand the evaporation behaviour of Urea-Water droplets.
- Following this the main results of the research were presented:
  - Sprays from small droplets ( $\leq 16 \mu\text{m}$ ) produce turbulent sprays which have greater mixing properties, while sprays from larger droplets ( $\geq 16 \mu\text{m}$ ) produce sprays which are laminar in nature, with minimal interaction with the surrounding gas.
  - While the mass of evaporated water shows monotonous reduction with respect to droplet size, the mass of evaporated Urea shows a dramatic reduction.
  - Preferential concentration of droplets in sprays could be observed by plotting joint PDF plots of parameters of interest and recognizing high density zones.
  - Three regions of preferential concentration were identified, and these regions affect rates of droplet evaporation. Colder regions, slow down the evaporation, while hotter regions accelerate the evaporation.

# Coolant Flow Modelling for Optimization of Thermal Management System Configurations

**Author:** Lassi Puolakka

**Keywords:** Thermal management systems, non-road mobile machines, hybrid powertrains, derivative-free solver, flow network analysis, configuration optimization

Thermal management has become increasingly important with the electrification and hybridization of non-road mobile machines (NRMM). With the introduction of power electronics, hybridization increases the number of components with distinct operating temperature requirements, increasing the complexity. Typical powertrain components requiring thermal management in hybrid NRMM and the respective nominal operating temperatures are presented in Figure 1. In addition, requirements for thermal management depend on the load cycle and ambient conditions. All these aspects introduce new challenges for the design of thermal management systems (TMS).

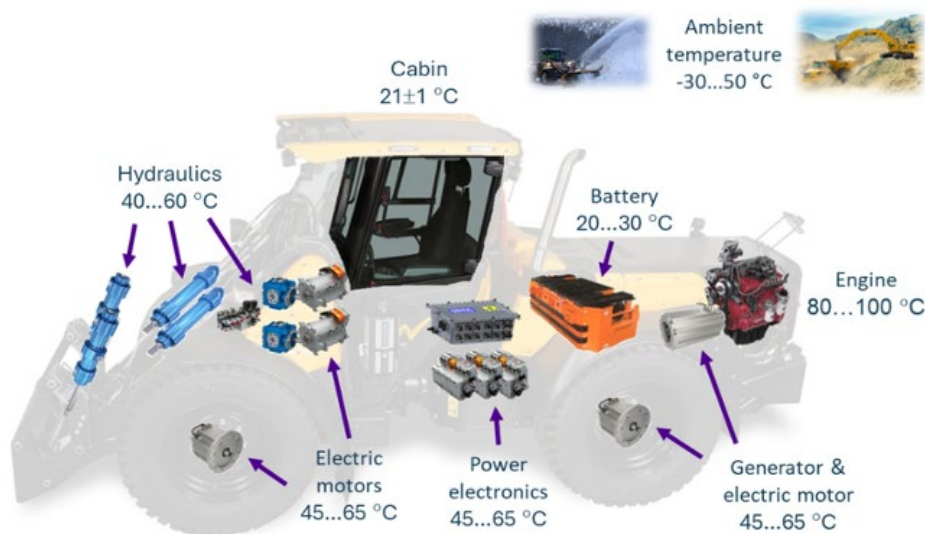


**Figure 1.** Components and nominal operating temperatures in hybrid NRMM

The main task of the TMS is to maintain the temperatures of the powertrain components within the desired limits. This both boosts performance by improving the efficiency available from the components and prolongs the lifetime of the components by reducing thermal degradation. In addition, the design of TMS should be viewed from the energy management perspective; by minimizing the energy consumption of the TMS, higher portion of the available energy can be used for useful work, increasing the overall efficiency and improving the fuel economy of the machine.

To account for these challenges and unlock the benefits, system-level configuration optimization of TMS must be applied. The task becomes very challenging as the number of feasible configurations increase super-exponentially with the number of distinct components in hybrid NRMM. For example, considering single-circuit liquid cooling, the number of feasible configurations for 11 components is in the magnitude of  $10^{14}$ . In order that as many configurations as possible can be evaluated, a computationally efficient solver for solving the coolant flow distribution was proposed.

The proposed  $K_v$  method is based on iteratively fitting the orifice flow coefficient equation  $Q=K_v \sqrt{\Delta p}$  to different parts of the system. The equation can be used to approximate the flow rate  $Q$  through and pressure drop  $\Delta p$  across an orifice. This is a good approximation for the pressure drop in TMS, since it is modelled as a second-order function of flow rate. The pressure drop in components is a second-order polynomial based on data sheets, and the hoses are modelled with the Darcy-Weisbach equation and Swamee-Jain friction factor. The effective flow coefficient  $K_v$  can be calculated for any series-parallel TMS configuration, making it possible to solve the flow distribution in arbitrary TMS configurations.

The proposed method is used to solve the flow distribution in an example TMS which represents the cooling system for the power electronics of the research platform sWille, a series-hybrid construction machine prototype. The cooling system includes five electric motors and inverters connected in total seven parallel lines, a radiator, and a coolant pump. The system is modelled as a flow network with nine edges and four nodes, which results in a total of 13 variables to be solved, including the flow rate in each edge and the pressure drop between each two adjacent nodes. The computational benefits of the method were compared against a Newton-based solver, which is common in industry-standard water network solvers. Newton is suitable, since the pressure drop in each edge is a monotone function of flow rate, and the Jacobian is a block matrix with diagonal dominance due to the nature of the problem. The computational results are presented in Table 1.

Method	$t$ [ms]	$n$	Speed-up factor
Newton	1.6	3	-
$K_v$ method	0.21	6	8.6

**Table 1.** Computational results from solving the example system.

The example system was solved by randomly changing the input flow from the coolant pump, and the computational times were averaged over 100 runs. Although requiring twice as many iterations, the proposed  $K_v$  method was on average 8.6 times faster than the well-established Newton's method. In addition, the  $K_v$  method is derivative-free unlike Newton, which requires the derivative of the pressure drop function in each edge. The proposed computationally efficient method for solving coolant flow distribution enables the use of system-level configuration optimization algorithms in the design of TMS.

Further work includes the calculation of coolant temperatures at each node assuming instant mixing of the inlet flows. Also, the characteristic curve of a centrifugal coolant pump should be included in the solver, since the total pressure drop in the system significantly affects the produced flow rate. Finally, the thermal models of powertrain components can be included, and the algorithm run with changing configurations to determine the optimal thermal management system configuration for a given NRMM and load cycle.

# Poster Session Highlights



# Multi-Parameter Model-based Optimization on NG-Diesel RCCI Combustion for a Medium Speed Marine Engine at 50% load

**Author:** Jeyoung Kim

**Keywords:** RCCI, VVA, marine engine, model-based optimization, multizone model

RCCI combustion is governed by multiple interacting parameters, including blend ratio, HRF injection strategy, boost pressure, and VVA. The growing number of control variables significantly expands the calibration and optimization space, leading to increased experimental time and cost. Model-based calibration and optimization offer an effective solution to this challenge by reducing the required experimental effort while maintaining accuracy.

In this study, an in-house developed thermo-kinetic multi-zone model, UVATZ, is used to capture RCCI combustion behaviour. The predictive combustion model is coupled with a GT-Power air-path model (figure1) to form an integrated simulation framework. This toolchain is first calibrated and validated against experimental data, demonstrating good agreement. It is then applied to perform multi-parameter optimization of engine performance and emissions.

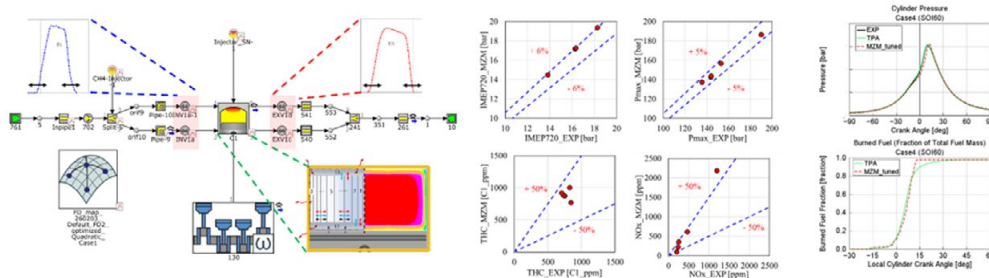


**Figure 1.** 1D engine model (left) and model validation with experimental data (right)

Model-based multi-parameter optimization was carried out at a 50% load operating point using the NSGA-III genetic algorithm, aiming to simultaneously maximize engine efficiency and minimize engine-out NOx emissions. A clear trade-off between indicated thermal efficiency (ITE) and NOx emissions was observed where reducing NOx requires retarding the combustion phasing (CA50), which in turn penalizes engine efficiency.

	Case4	ITE720 [-]	BR [-]	SOI [BTDC]	Pintake [bar]	Lambda [-]	VVA [CAD]	Pmax [bar]	MPRR [bar/deg]	ISNOx [g/kWh]	ISTHC [g/kWh]
OP1	Baseline	--	0.908	60	2.4	2.08	--	155.7	7.111	1.518	2.232
OP2	Optimized wo VVA (Max. ITE & Min NOx)	+2.0%	0.8779	79	2.764	2.431	--	167.2	8.396	0.3206	2.4226
OP3	Optimized with IV (Max. ITE & Min NOx)	+2.5%	0.8779	78	2.826	2.598	IVO-1 IVC: Miller+8.5	178.1	8.491	0.1814	2.9195
OP4	Optimized with EV (Max. ITE & Min NOx)	+2.0%	0.8751	62	2.8675	2.6789	EVO-6 EVC:16ATDC	165.4	5.233	0.3145	2.9304
OP5	Optimized with VVA (Max. ITE & Min NOx)	+2.8%	0.8774	70	2.8312	2.6850	IVC:Miller+14.5 EVO-10 EVC:1.86ATDC	193.1	9.023	0.2858	2.879

**Figure 2.** Optimization results



Different optimization results are compared (figure 2). Most cases improved ITE720 more than 2 %. Mainly, the baseline point has rather delayed combustion phase. By optimizing the combustion phase (CA50) close to TDC, it has better ITE 720. In order to advance combustion phase, VVA's thermal effect using IVC is utilized in the optimization.

Blend ratio (BR) is the dominant factor governing indicated thermal efficiency (ITE), NO<sub>x</sub> emissions, maximum cylinder pressure (P<sub>max</sub>), and pressure rise rate (PRR). VVA's impact is rather secondary but its role is not trivial. VVA provides an additional efficiency improvement of approximately +0.8% using thermal effect. In the end, the optimized VVA achieves 2.8% higher thermal efficiency with low NO<sub>x</sub> emissions below EU stage-V limit without exceeding engine design limits (P<sub>max</sub> < 225 bar and MPRR < 10 bar/deg).

This study demonstrates that VVA can effectively enhance RCCI engine performance and emissions simultaneously and highlights its importance as a key enabler for next-generation multi-fuel combustion engines.



# Reactivity Recovery in Low-Load NG–Diesel RCCI Using NVO Diesel Injection

**Authors:** Amir Soleimani, Jacek Hunicz, Jeyoung Kim

**Keywords:** Negative valve overlap (NVO), in-cylinder fuel reforming, recompression thermochemistry, reactivity-controlled compression ignition (RCCI), dual-fuel (DF) combustion

## Main idea and objective

Low-load NG–diesel RCCI operation in medium-speed marine engines is limited by weak in-cylinder thermal conditions, leading to incomplete NG oxidation, unstable combustion, and increased methane emissions. NVO diesel injection was investigated as a way to recover combustion efficiency by improving the thermal/reactive state during recompression.

## Approach

A simulation-based study was performed using experimental reference data from a Wärtsilä 6L20 dual-fuel RCCI research engine. The UVATZ multi-zone model was extended for variable valve timing and NVO recompression. A near-misfire baseline was created by lowering intake temperature, and this condition was used to assess the effects of NVO injection timing and ratio.

## Main findings

The effect of NVO diesel injection strongly depends on timing. As shown in Fig. 1, Pre-TDC injection gave the clearest combustion-efficiency recovery because part of the injected fuel oxidized during recompression, increasing the next-cycle intake-valve-closing temperature and supporting the main combustion event. Near-TDC injection gave the weakest response, as diesel was mainly converted into CO and hydrocarbon fragments with limited useful reactivity. Post-TDC injection mainly carried fuel into the next cycle, with recovery observed only at lower NVO injection ratios. Overall, NVO diesel injection can improve low-load NG–diesel RCCI combustion, but only within a suitable timing and ratio window.

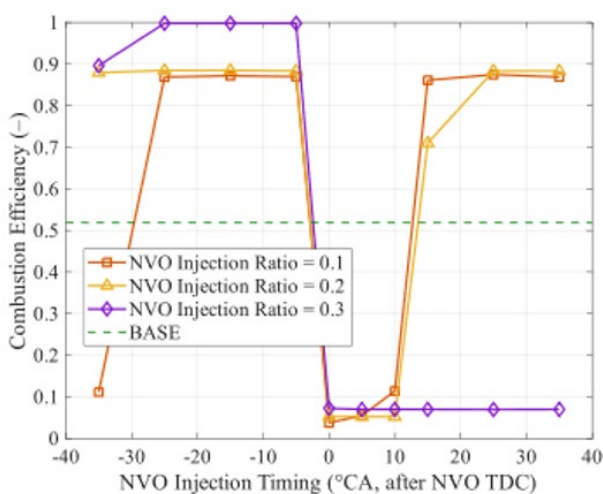


**Figure 1.** Effect of NVO diesel injection timing and ratio on combustion efficiency

# Optimization of Emission Catalyst Solutions for Methanol, Ammonia and Methane Marine Engines – Towards Coordinated RCCI+ATS Design

**Authors:** Jan Němec, Teuvo Maunula

**Keywords:** Ammonia, methanol, methane, SCR, emissions, RCCI, marine

Marine propulsion aims for carbon neutrality by 2050, requiring new dual fuel engines and advanced aftertreatment systems. This research focuses on methanol (MeOH), methane (CH<sub>4</sub>), and ammonia (NH<sub>3</sub>) fuels, using modelling tools to design catalysts that reduce greenhouse gas and pollutant emissions.

## Methods

1D transient and steady state modelling was performed with GT Suite. Simulations used extruded vanadium based SCR (V SCR), dual layer ammonia slip catalyst (ASC), and methane oxidation catalyst (MOC). Reaction kinetics and pore diffusion limitations were included, supported by data from dual fuel engine simulations.

**SCR and NH<sub>3</sub> slip catalyst:** NH<sub>3</sub> fuelled engines produce higher raw NO<sub>x</sub> and NH<sub>3</sub> emissions, demanding efficient NO<sub>x</sub> conversion and control of NH<sub>3</sub> slip. A small ASC after V SCR improves deNO<sub>x</sub> efficiency without excess NH<sub>3</sub> slip. NH<sub>3</sub> adsorption on V SCR buffers emissions but affects transient NO<sub>x</sub> conversion. Proper SCR+ASC design also promotes the oxidation of methanol, CO and formaldehyde (HCHO) emissions from methanol engines.

**Methane oxidation catalyst:** MOC removes CH<sub>4</sub> (greenhouse gas) emissions from methane engines. Hydrocarbons, especially CH<sub>4</sub>, are harder to oxidize than CO or HCHO. NO<sub>2</sub> formation within MOC promotes SCR reactions. Higher pressure and temperature before the turbocharger may enhance CH<sub>4</sub> oxidation and reduce activation temperature.

## Conclusions

- Simulations and experiments show increased NO<sub>x</sub> conversion and reduced NH<sub>3</sub> slip with SCR+ASC systems.
- Methanol and formaldehyde are efficiently removed, while ASC ensures complete CO oxidation.
- TiO<sub>2</sub> based SCR catalysts buffer NH<sub>3</sub> tail-pipe emissions below 250 °C.
- Pt ASC after V SCR promotes NH<sub>3</sub> removal under transient conditions with high efficiency in NH<sub>3</sub> engine application (NH<sub>3</sub> from engine and urea).
- MOC benefits from elevated pressure and temperature in pre-turbo location, supporting methane oxidation.
- Further experimental data will be utilized to refine models in future.
- The ultimate goal is integrated simulation of engine and catalytic aftertreatment systems for carbon neutral marine propulsion.

# Variable Valve Actuation on RCCI Combustion and Emission Characteristics in a Medium Speed Marine Engine

**Author:** Jeyoung Kim

**Keywords:** RCCI, VVA, EHVA, thermal effect, marine engine, compression temperature

Reactivity-controlled compression ignition (RCCI) combustion is highly sensitive to in-cylinder temperature which strongly influences auto-ignition of high-reactivity fuel (HRF), chemical reaction rates, and overall combustion phasing. In low-temperature combustion concepts such as homogeneous charge compression ignition (HCCI), partially premixed compression ignition (PPCI), and RCCI, intake temperature control has commonly been used to regulate combustion. However, this approach typically requires additional thermal conditioning hardware and exhibits slow response times.

Fully flexible variable valve actuation (VVA) systems offer a more responsive alternative by enabling rapid control of in-cylinder temperature by adjusting valve timing and lift. In this study, a comprehensive VVA sweep was conducted, including intake valve opening (IVO), intake valve closing (IVC), exhaust valve closing (EVC), and valve overlap (VO). Experiment was performed on a medium-speed marine engine equipped with an electro-hydraulic valve actuation (EHVA) system (Figure 1).

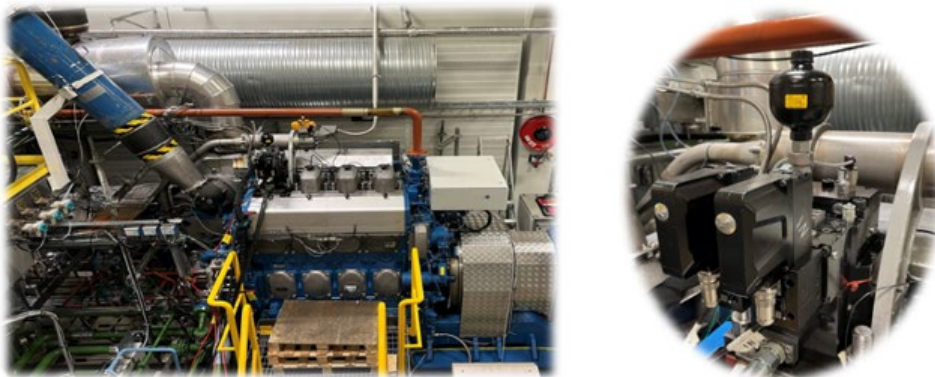


**Figure 1.**  
Research engine platform (left) and EHVA system (right)

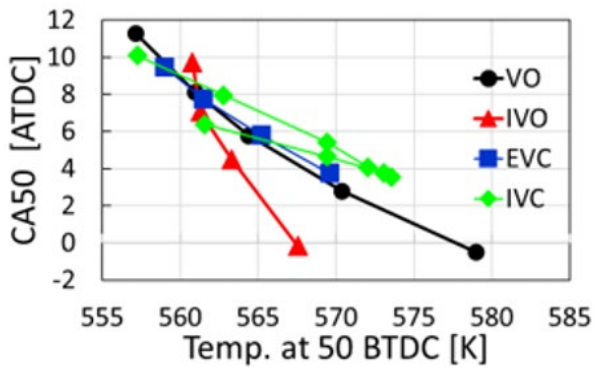


**Figure 2.**  
VVA's thermal effect on RCCI combustion

The results (Figure 2) demonstrate the strong thermal influence of VVA on RCCI combustion. As compression temperature increases across all VVA strategies, the combustion phase (CA50) consistently advances. However, the sensitivity of this response varies between strategies due to differences in their underlying temperature control mechanisms.

EVC and VO primarily increase in-cylinder temperature by retaining hot exhaust gases—an effect equivalent to internal exhaust gas recirculation (i-EGR)—resulting in similar response gradients. In contrast, IVO influences temperature through in-cylinder heat transfer, while IVC modifies charge density and effective compression ratio to regulate compression temperature.

Overall, VVA provides a flexible and effective means of controlling RCCI combustion. It can serve as an additional control parameter alongside conventional control variables such as blend ratio, HRF injection timing, and lambda.



# Cost-Aware Multi-Step Design for BlackBox Function Mapping via ARD-Based Gaussian Processes

**Authors:** Md Shahnawaz Ahmed, Anders Brink

**Keywords:** Sequential DoE, gaussian process regression, ARD, active learning, informative path planning

This poster presents a cost-aware, forward-looking approach for mapping expensive black-box engineering systems such as modern maritime shipping engines. These systems are hard to approach since their input–output relationships are unclear, experiments are costly, and for such systems it is impractical to research in entirety due to the extensive number of high-dimensional operating spaces.

Data collection through Classical Design of Experiments (DoE) is structured. Yet it is often greedy. It chooses the next experiment without adequately accounting for what effect a decision today will have on future measurements. In ship-engine testing, this limitation is especially important because moving between engine operating states has a physical transition cost.

The proposed framework combines Gaussian Process Regression (GPR) with Automatic Relevance Determination (ARD), cost-aware multi-step design, and informative path planning. GPR provides both predicted responses and uncertainty estimates, while ARD learns which input variables are most relevant. A receding-horizon strategy then plans experiment sequences that balance information gain against the cost of state changes.

**Key idea:** plan a sequence of experiments that maximizes learning about the global response surface while minimizing unnecessary and costly transitions between engine states.

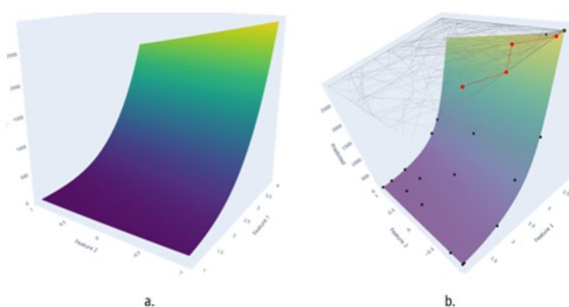


**Figure 1.**

Synthetic Rosenbrock steep-wall surface. The plots compare the true response surface with the surface constructed after planned experiments. The red dashed route marks a planned high-information path, and black dots indicate previous observations.

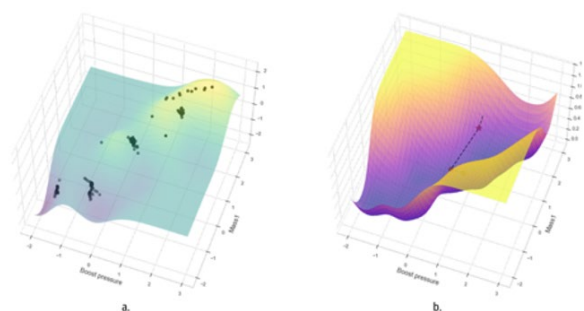


**Figure 2.**

Previous experiments using RCCI engine data. The fitted model uses existing experimental points, while the variance plot shows the planned future path, batch experiment settings, and the next experiment location marked with a star.

# Numerical Study of n-heptane / Methanol Dual Spray Interaction in Compression Ignition Environments

**Authors:** Bishal Shrestha, Qiang Cheng, Ahmad Zeeshan, Viljam Grahn, Jari Hyvönen, Shervin Karimkashi, Ossi Kaario

**Keywords:** Ignition delay time (IDT), spray interaction, LES (large-eddy simulation), OpenFOAM, Cantera

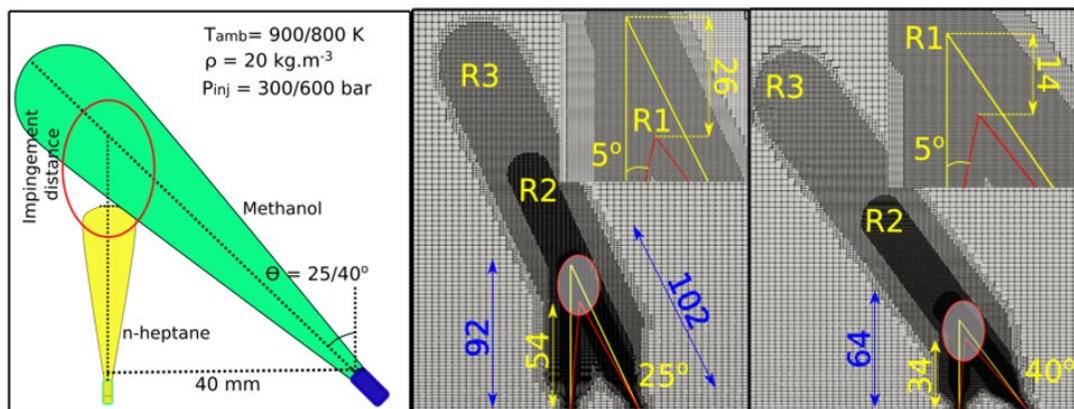


**Figure 1.** Schematics (left) and mesh setup (right) of the methanol and n-heptane spray.

Case	Injection Angle [°]	Injection Pressure [bar]	Temperature [K]	Impingement distance [mm]	IDT (methanol) [ms]	
					LES	Exp
I	25	600	900	54 - 80	1.27	1.15
II	40	600	900	34 - 48	0.61	0.7
III	40	300	900	34 - 48	0.60	0.59
IV	25	600	800	54 - 80	1.75	n/a
V	40	600	800	34 - 48	1.83	n/a

**Table 1.** The operating conditions and its corresponding ignition delay time of methanol.

The current study aims to analyse the combustion characteristics of methanol and pilot n-heptane and validate with the OSCC experiments. Figure 1 features the schematics of spray location and orientation, operation conditions, and mesh setup. Additionally, in Figure 1,  $R1(dx) = 125 \mu\text{m}$ ,  $R2 = 250 \mu\text{m}$ ,  $R3 = 500 \mu\text{m}$ , and  $dx \neq dy = dz$ . Spray D and H injection profiles from ECN were adopted for methanol and n-heptane sprays, respectively. Mass flow rate for methanol  $m_{me} = 0.14$  and  $0.07 \text{ kg/s}$  at 600 bar and 300 bar respectively, while mass flow rate for n-heptane  $m_{c7} = 0.007 \text{ kg/s}$  at 800 bars. The effect of injection pressure, temperature, and injection angle on ignition delay time (IDT), Flame lift-off length (FLOL), emission was studied.

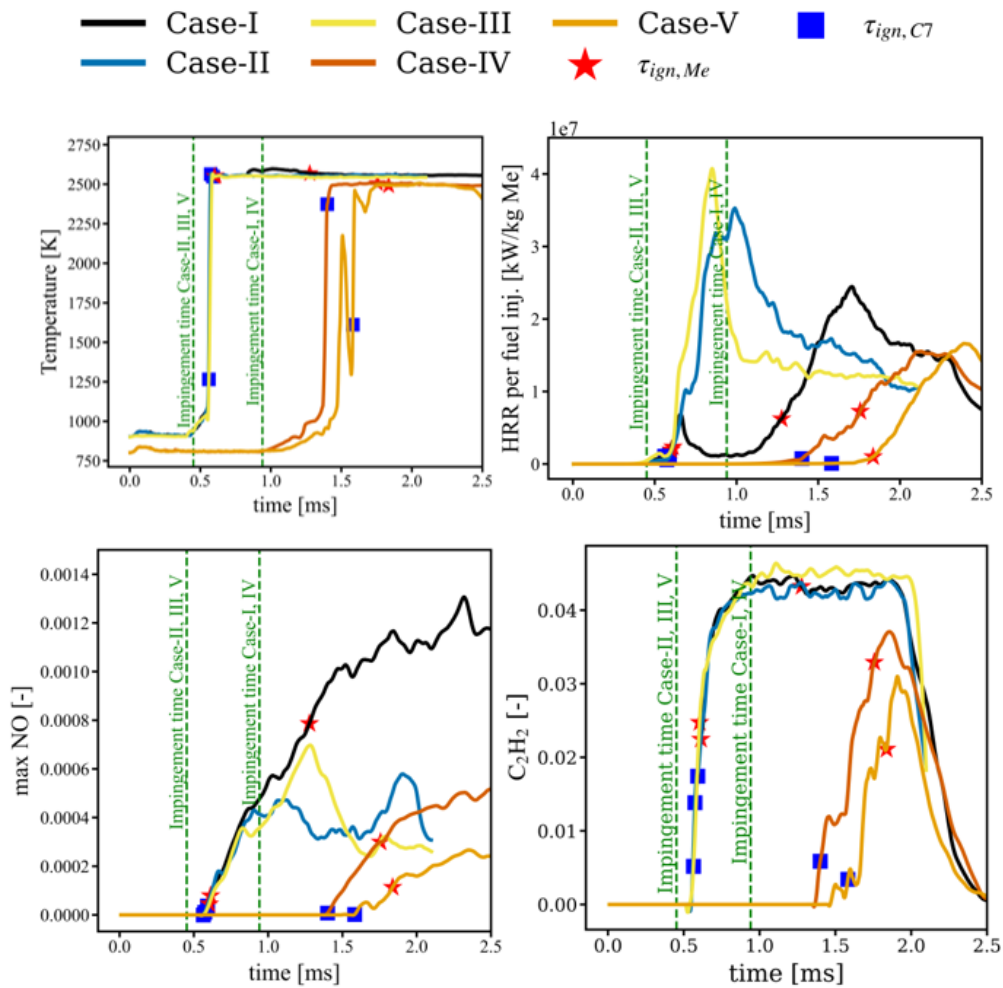


**Figure 2.** Temperature, Heat release rate (HRR), NO and Soot (C<sub>2</sub>H<sub>2</sub>) emissions, impingement time (-), and ignition delay time (IDT) for n-heptane (■) and methanol (★) for all cases.



# Hot-source Pre-ignition in H<sub>2</sub>-enriched Reactivity Controlled Compression Ignition Marine Engine

**Authors:** Kian Golbaghi, Jari Hyvönen, Ossi Kaario, Maciej Mikulski

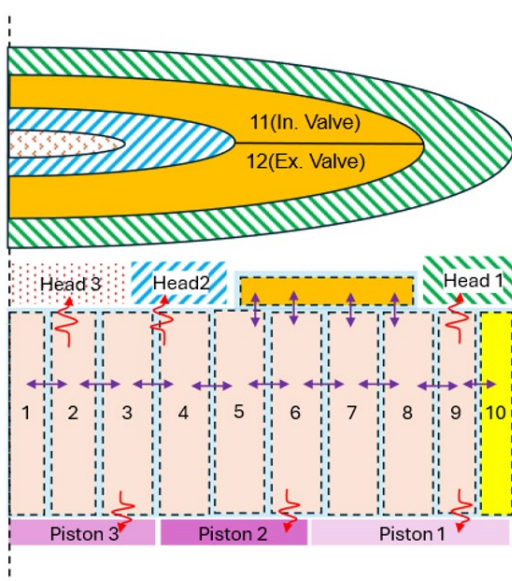
**Keywords:** RCCI, hydrogen enrichment, marine engines, multi-zone modelling, pre-ignition

## Abstract

Hydrogen (H<sub>2</sub>) enrichment in dual-fuel Reactivity Controlled Compression Ignition (RCCI) marine engines is increasingly viewed as a viable route toward 55% thermal efficiency and substantial reductions in carbon-based emissions. Yet several practical limitations, such as component thermal loading and NO<sub>x</sub> control, restrict the allowable H<sub>2</sub> fraction, particularly under high-load conditions. Amongst the limiting phenomena, pre-ignition triggered by localized hot surfaces remains insufficiently addressed by existing simulation frameworks, thereby restricting the use of Model-in-the-Loop engine calibration strategies.

This study applies an advanced performance-oriented multi-zone combustion model to investigate natural gas–hydrogen mixtures serving as the low-reactivity fuel in a large-bore RCCI engine. To capture the thermal impact of engine components, a detailed wall heat transfer solver is integrated into the model. The approach uses a boundary-layer formulation that couples transient wall temperatures to the adjacent gas zones, enabling a more realistic representation of local temperature gradients and their role in premature ignition.

The modelling framework is validated against reference natural gas–diesel operating points, demonstrating consistent reproduction of global combustion behaviour and emissions trends. Following validation, high-load operation is analysed by progressively increasing the H<sub>2</sub> fraction to assess the sensitivity of phasing stability and pre-ignition to fuel composition and wall-temperature distribution.



## Highlights

The temperature gradient within the cylinder gas was improved by assuming boundary zones with fixed temperature.

Boundary layer size was tuned to reproduce emission results.

Detailed thermal analysis shows a smoother yet faster progress of the combusting zones in the H<sub>2</sub>-enriched case.

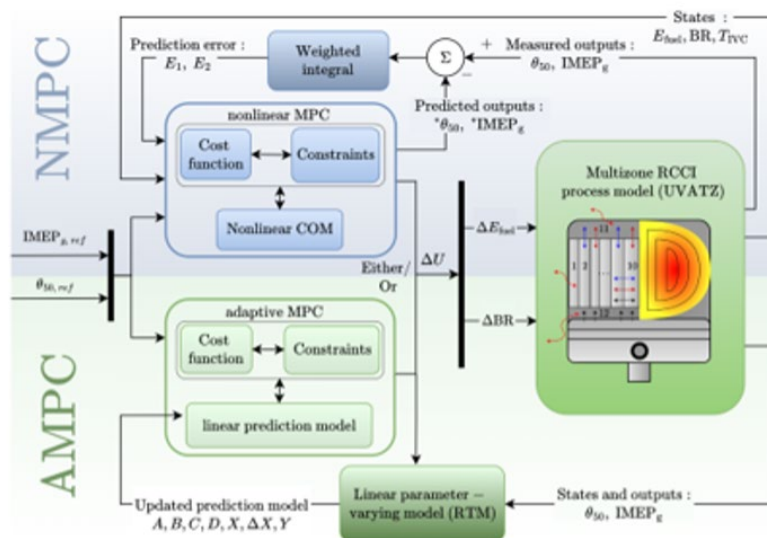
**Figure 1.** The zonal configuration of UVATZ with respect to thermal boundary regions

# Model-based Predictive Control of RCCI Engine Combustion

**Authors:** Jeremias Pohjola, Amir-Mohammad Shamekhi, Amin Modabberian

**Keywords:** Combustion control, MPC, marine, RCCI, simulation

This study targets combustion control of marine RCCI engines by adjusting fuel injection to regulate combustion timing and power, comparing two model predictive strategies: adaptive MPC (AMPC) and nonlinear MPC (NMPC). RCCI delivers ultra-low NO<sub>x</sub> and soot with high efficiency but is difficult to control due to strong coupling and nonlinearity; model predictive control addresses this by predicting engine behaviour over a horizon, enforcing constraints, and optimizing future actions. AMPC employs a piecewise linear, adaptively updated model for speed and computational efficiency, while NMPC uses a full nonlinear model better suited to highly coupled, strongly nonlinear dynamics. Both controllers regulate IMEP and combustion phasing (CA50) by adjusting total fuel energy (E<sub>fuel</sub>) and blend ratio (BR), with a decentralized PI framework used as a baseline. NMPC leverages prediction error to refine its model online, improving accuracy under disturbances; AMPC uses a real time model (RTM) for state estimation and periodic re linearization. MIL simulations with transients between calibrated mid and high load points and unstructured uncertainties confirmed stable performance and effective constraint handling on actuators and combustion metrics. Both strategies achieved accurate CA50 and IMEP tracking with efficient fuel use; NMPC was more robust to nonlinearities and mismatches, whereas AMPC responded faster and required less computation. The frameworks are implemented on an RCP platform, enabling upcoming EIL testing and indicating strong potential for real engine deployment and scalable control of multi fuel, multi input RCCI systems.



# Development of Multi-Cylinder Methanol Engine with EHVA

**Authors:** Tino Tuominen, Rasmus Pettinen, Markus Rumjantsev

**Keywords:** Methanol, EHVA, VVA, SI combustion

## Background

Currently, there is no CO<sub>2</sub> regulation for non-road mobile machine (NRMM) sector. However, it is certain that there will be one introduced in the upcoming years. To fulfil the future emission regulations, sustainable fuels are part of the solution. Multi-cylinder combustion engine (MCE) with fully variable electro-hydraulic valvetrain (EHVA) will work as a flexible platform for investigating different types of fuels together with advanced combustion technologies and control strategies.

During Flex-CPT (WP2, Task 2.2.4), the MCE will be used for investigating the true potential methanol spark-ignited (SI) combustion. EHVA enables the possibility to freely investigate the impact of different valve timings. For example, compression ratio can be dynamically varied for different load cases to optimize engine efficiency and simultaneously mitigate knocking in SI combustion. The MCE engine is based on a modern 4-cylinder NRMM diesel engine, AGCO Core 50. Being a diesel engine, dedicated modifications are required to facilitate SI-combustion.

## EHVA Valvetrain

The EHVA valvetrain (Figure 1) consists of a control system implemented on Speedgoat and a custom-made hydraulic block fitted on top of the cylinder head. The hydraulic block contains 8 hydraulic pistons which are used as pushrods directly above the intake and exhaust valves. The pistons are operated with proportional hydraulic valves together with closed loop feedback from position transducer placed on top of each piston.

The control algorithm consists of two separate controls: a simple P-controller for amplifying the control signal working together with an additional iterative controller. The iterative controller uses the error from previous working cycle to correct the demanded valve control signal for the next cycle. Each intake and exhaust valve pairs are corrected independently, and accuracy of this control system is excellent. Depending on engine speed, the error between demanded and measured valve lift is mostly between 0.1 to 0.2 mm, Figure 2.



**Figure 1.** EHVA system under testing with cylinder head

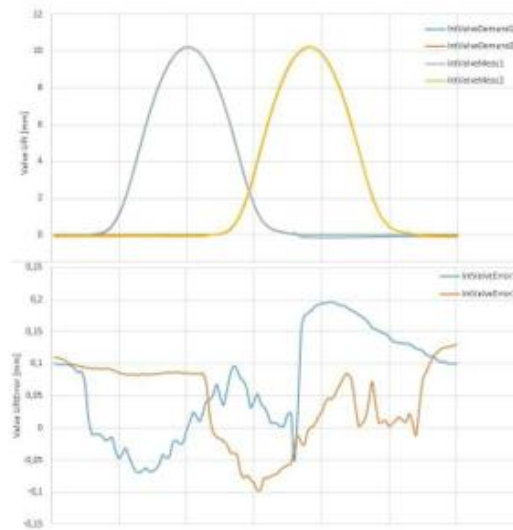


**Figure 2.** Example of EHVA performance at 800rpm

### Engine hardware modifications.

Using diesel engine as basis for SI-engine requires modifications in many aspects. As conventional SI-engine runs with lower compression ratio (CR) than a diesel engine, new pistons were acquired.

The methanol combustion will be investigated with port fuel injection (PFI) hence the original cylinder head design needed modifications in the raw casting as well. Since the original cylinder head has an integrated intake manifold in it, there was no way to directly mount the PFI injectors to the manifold. Hence, special injector adapters were designed.

Naturally, spark-plugs are needed for SI-combustion thus they have dedicated machining at the centre of the cylinders. For fixing the fuel injections equipment (FIE), a dedicated bracket was designed and manufactured. Lastly, a new intake throttle valve (ITV) body required an adapter for installing it to the intake manifold.

# Development of 1D Modelling Tools for Studying Methanol Evaporation

**Author:** Rasmus Pettinen

**Keywords:** Methanol, evaporation, PFI, simulation, NRMM

The purpose of the work was to further investigate the evaporative properties of methanol and identify solutions for extending its use in (PFI-SI) NRMM applications. In addition, the objective was to develop a numerical model that enables efficient screening of key hardware configurations and operating parameters, supporting a deeper understanding of methanol as an advanced fuel.

Adequate fuel evaporation is essential for proper engine performance, particularly during cold starts, low-temperature conditions, and transient operation. Compared to conventional spark-ignition fuels, methanol exhibits less favourable evaporation behaviour, which can lead to challenges in combustion. Insufficient evaporation and improper spray characteristics may result in wall wetting, unburned fuel, reduced efficiency, and increased emissions. However, methanol's high latent heat of evaporation (ca. 1100 kJ/kg for methanol compared to ca. 250 kJ/kg for Diesel), when effectively utilized, can enhance overall engine performance by improving charge cooling and in-cylinder thermal conditions.

The work initially focused on using the 1D GT-Power simulation tool. Due to limitations within the GT toolset in modelling fuel evaporation processes, a complementary model was developed. This model integrates GT-Power derived engine data with classical numerical approaches and accounts for droplet-, wall film-, and in-cylinder evaporation. The model incorporates several key inputs, including effects of fuel enrichment (air-to-fuel ratio), droplet size, fuel pressure, and the motion of droplets and charge. It also considers charge, fuel, and intake port temperatures, as well as intake and compression effects. Additional parameters such as compression ratio and turbulence are included to capture their influence on evaporation behaviour.

An initial version of the model has been completed. At its current stage, various methods and solutions have been evaluated to improve evaporation efficiency. The results indicate that, in port fuel injection (PFI) systems, fuel enrichment during cold starts is necessary to ensure sufficient fuel ignitability. The initial results indicate that fuel evaporation can be improved through preheating of the fuel, intake air, or surrounding components, reducing droplet size, and increasing the compression ratio. However, the model is not yet calibrated or validated and will undergo further development within FCPT WP2, Task 2.2.4.

## Additional information

This work was carried out as part of a three-month research exchange from VTT to the Lund University (LTH) Combustion Engine Division. VTT acknowledges the support received from the LTH combustion engines division throughout the project. In parallel with this study, Aalto University conducted 3D CFD simulations of PFI methanol injection in similar engine applications.

# Results from the Engine Experiments with Methanol-RD-Oc Fuel Blends

**Authors:** Huaying Wang-Alho, Ossi Pohjolainen, Md Rakin Tajwar, Teemu Ovaska, Katriina Sirviö, Maciej Mikulski, Giacomo Belgiorno, Jacek Hunicz

**Keywords:** Combustion, alternative fuels, engine emissions, methanol, internal combustion engines, compression ignition engines

## Drop-in blends in CI

The novelty of this research was to study methanol/ renewable diesel/1-octanol (MeOH–RD–Oc) drop-in -blends against diesel in a compression-ignited (CI) high-speed non-road engine, which was equipped with advanced combustion and aftertreatment system technologies. Drop-in operating strategy using standard diesel calibration enables to easily transform from fossil fuels to renewable. The study aimed to find the effects of methanol blends on combustion, emissions, and efficiency using three operating points of the Non-Road Steady Cycle.

## Results – Reductions in raw emissions observed.

Main findings were reduction raw emissions, and slight increase on some load points. The total particle number (TPN) above 23 nm was reduced in all load points. At low load, methanol blends reduced nitrogen oxide (NO<sub>x</sub>) emissions. At high load, a moderate increase in NO<sub>x</sub> of up to 2% occurred, maintaining compliance with Tier 4 emission requirements (Figure 1a). Carbon dioxide (CO<sub>2</sub>) emissions were reduced from the diesel baseline (Figure 1b).

Other significant findings were that alcohol blend fuel as drop-in resulted with similar combustion and emission behaviour and similar or better BTE, especially at low load (Figure 1c). Additionally, engine power was equivalent to the diesel baseline. Peak pressure was enhanced with methanol blends, especially at low load, thanks to its higher premixed combustion ability.

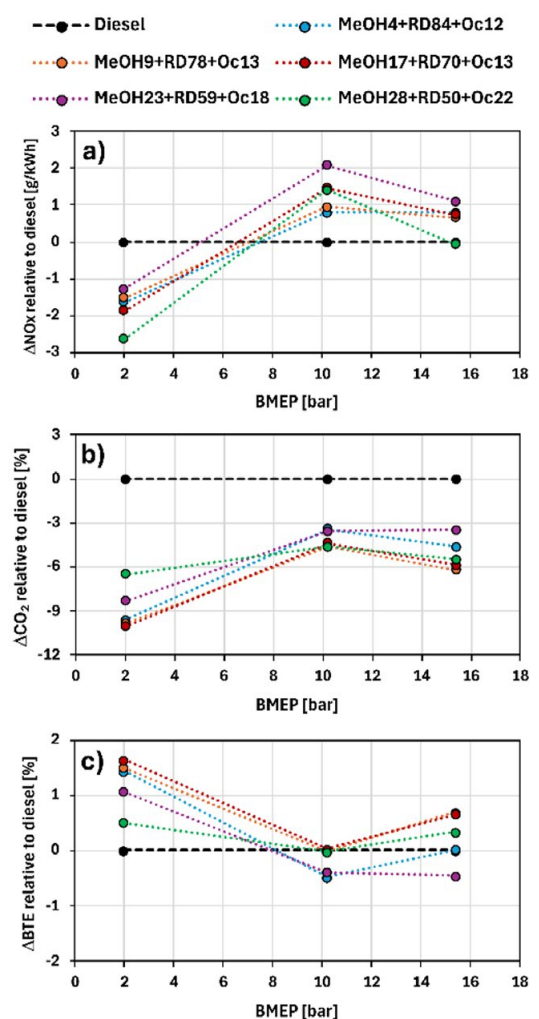
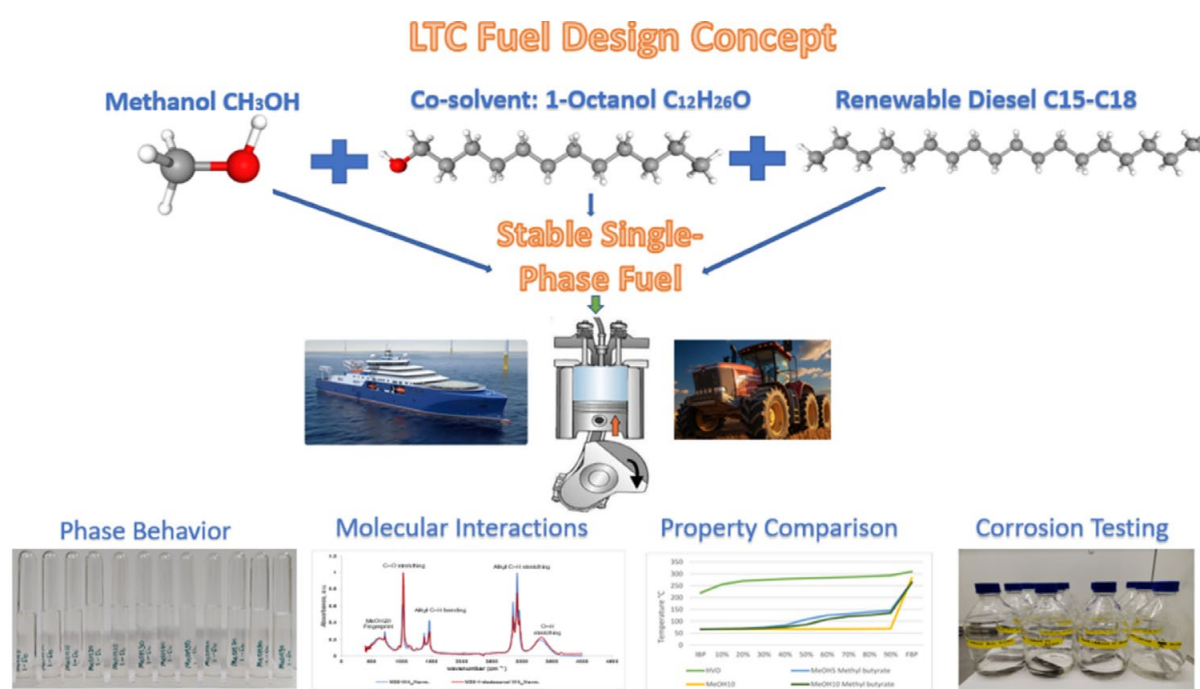


**Figure 1.** The relative change of a) NO<sub>x</sub>, b) CO<sub>2</sub> and c) BTE of studied fuel blends compared to diesel at 1500 rpm.

# Development and Validation of Methanol and Renewable Diesel Blends as Low-Temperature Combustion Fuels

**Authors:** Huaying Wang-Alho, Fatimoh Balogun, Carolin Nuortila, Katriina Sirviö

**Keywords:** Methanol; renewable diesel; co-solvent; blending; CI engine; low-temperature combustion



## Summary

Low-temperature combustion (LTC) requires fuels with controllable reactivity and high oxygen content to simultaneously achieve high efficiency and low emissions. Methanol and renewable diesel (RD) represent a promising fuel combination, integrating the clean combustion characteristics of oxygenated fuels with the high ignition quality of diesel-type fuels. However, their intrinsic immiscibility limits direct application, necessitating the use of suitable co-solvents to stabilize the blends.

This work systematically investigates the role of oxygen-containing co-solvents in promoting miscibility between methanol and renewable diesel. The study focuses on understanding co-solvent-assisted miscibility, molecular interaction mechanisms, evaluating fuel physicochemical properties, and assessing material compatibility with engine-relevant metals.

The results demonstrate that co-solvents are essential for achieving stable single-phase blends. Among the tested candidates, 1-dodecanol exhibited the strongest solubilizing capability, followed by 1-octanol, while methyl butyrate showed the weakest performance. Higher alcohols were found to enhance miscibility by balancing intermolecular forces and stabilizing hydrogen-bonding interactions. The addition of co-solvents modifies fuel properties, increasing density and reducing viscosity, while still maintaining values within acceptable ranges for compression-ignition (CI) engine applications.

Compatibility tests indicate that renewable diesel and stabilized blend fuels show good corrosion behaviour with common engine metals, whereas pure methanol exhibits slight dissolution effects on aluminium and zinc. Furthermore, ignition delay measurements reveal a strong Arrhenius-type temperature dependence, with ignition delay times decreasing monotonically as temperature increases and spanning approximately 25–3500  $\mu\text{s}$  over the range 1150–1550 K.

Overall, the combined molecular, physicochemical, and material compatibility analyses provide strong evidence supporting the feasibility of methanol–renewable diesel–co-solvent blends as alternative fuels for low-temperature combustion. Future work will focus on engine-level validation, including combustion performance, efficiency–emission trade-offs, and particle emission characteristics under realistic operating conditions.

# Laboratory Method for Analysing Fuel and Material Compatibility

**Authors:** Katriina Sirviö, Carolin Nuortila, Huaying Wang-Alho, Jonna Kaivosoja, Fatimoh Balogun, Iida Sieranen

**Keywords:** Material compatibility; immersion test; alternative fuels; analytical method; laboratory method development

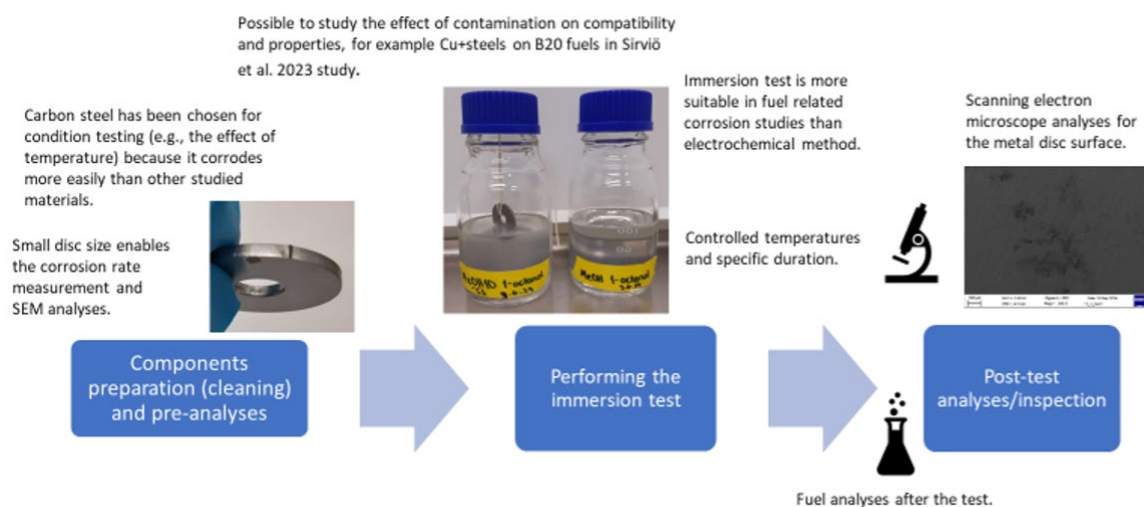


**Figure 1.** Immersion test is a step-by-step process.

## Summary

In the University of Vaasa Fuel laboratory, several tests have been conducted to evaluate fuel and fuel blend material compatibility. The studies have been immersion tests, and every study has provided new insights which can develop further the method.

Wang-Alho et al. (2024) investigated both methanol and renewable diesel, and their blends (50:50 % share on energy) with and without additives. Fuel-material compatibility with carbon steel, stainless steel, special alloy (tempering) steel and aluminium was studied for 2 months. The blends showed good compatibility with the chosen materials, with neat methanol showing a slight dissolving effect on aluminium (dissolving Al) and carbon steel (dissolving Zn).

The study by Kaivosoja et al. (2024) focused on evaluating hydrochloric acid (HCl) contamination of light fuel oil on carbon steel, stainless steel, special alloy (tempering) steel and aluminium. The samples were exposed to contamination for approximately one month. HCl caused severe corrosion, even though it did not have an effect on fuel properties. Even 25 ppm HCl contamination caused a degree of corrosion.



The study by Sieranen (2025) aimed at improving the Fuel laboratory's immersion test's experimental design. The second aim was to implement the improved immersion test and examine the corrosion caused by renewable diesel, methanol, a fuel blend (RD 78 %, MeOH 8 % and 1-octanol 14 %) and light fuel oil in carbon steel and examine the effect of temperature on corrosion for approximately 12 days. The study showed that at temperatures of 23 C and 40 C, the immersion tests had minor or no effect on the results. In the chosen conditions none of the fuels caused corrosion.

Nuortila et al. (2025) investigated the corrosion propensity of carbon steel discs immersed in pure methanol and in a methanol-HVO-1 octanol blend. The blend consisted of methanol 71%, HVO 7%, 1-octanol 22%, energy basis. The experiment lasted for 20 days. The results showed no signs of corrosion on the tested carbon steel quality.

Currently the method is developed further with upgraded pyrolysis lignocellulosic oil in the FOR-BLEND project, enabling us to better meet the broad range of fuels. The immersion test describes the compatibility of the fuel system, material, and fuel under normal pressure and at the temperature specified in the test (Yong H. et al. 2024). To better understand the corrosion risks caused by methanol combustion, a more complex test matrix must be considered. Many parts of a marine engine operate in an environment with high temperature and high pressure, where combustion products of fuels are present (Yong C. et al. 2025). Understanding this entity requires high-temperature and high-pressure conditions formed by the combustion products of alternative fuels in order to study their effects on the corrosion behaviour of engine materials. For future work, the aim is to evaluate the relevance of higher temperatures and higher-pressure studies in our laboratory.



# Evolution of Thermal Gradient in LH2 Tanks Subjected to Motion

**Authors:** Anna Pakarinen, Anders Brink

**Keywords:** Computational fluid dynamics, liquid hydrogen, ullage, thermal gradient, ship motion

For liquid hydrogen tanks used in ships, the quality of thermal insulation and ship motions affect heat ingress into the liquid and subsequent boil-off generation. At steady state conditions, the vapor in the tank becomes thermally stratified while the liquid is saturated. Applying motion to the tank leads to mixing in the ullage and increased heat transfer from vapor to liquid, which leads to more liquid boil-off.

In this study, the thermal gradient in the ullage space of an LH2 tank subjected to rolling motion has been investigated using Computational Fluid Dynamics. Cases with different thermal boundary conditions were studied where the temperature distribution in the vapor was computed for stationary and dynamic conditions. The thermal gradient at different points of tank motion for one of the studied cases is shown in Figure 1.

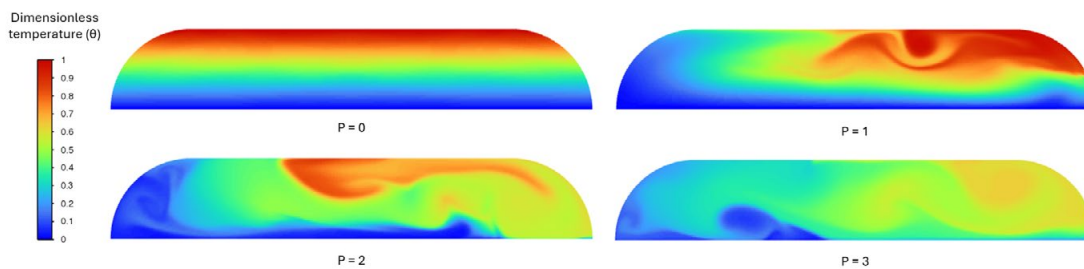


**Figure 1.** Dimensionless temperature distribution in the ullage of the partially filled LH2 tank after  $P = 0, 1, 2$  and  $3$  (pe-riods of tank motion).

At stationary conditions the thermal gradient is linearly increasing in the vertical direction with warmer vapor layers settling in the upper part of the tank. As the tank is subjected to motion, different vapor layers begin to mix with each other, and the warm vapor comes into contact with the liquid surface and wetted tank walls. Over time, more heat is transferred into the liquid and the vapor becomes destratified, reaching a uniform temperature distribution.

In the study, it was also observed that when the initial thermal gradient is large, the difference in density between upper and lower vapor layers restricts mixing, which causes the vapor to separate into cold and warm zones. The heavier cold vapor stays at the bottom and prevents the warm vapor from reaching the liquid surface and wetted tank walls, slowing down heat transfer to the liquid.

# Impact on Biofuel-Derived Impurities on NH<sub>3</sub>-SCR Catalyst Performance

**Authors:** Tytti Ristikaarto, Mika Huuhtanen, Teuvo Maunula

**Keywords:** Catalyst poisons, catalyst deactivation, bio-based fuels, Fe-SCR, Zeolite Beta, Multicomponent poisoning

In this study was investigated how impurities originating from biofuels affect the performance and deactivation on Fe-based NH<sub>3</sub>-SCR catalysts used for NO<sub>x</sub> removal in exhaust after-treatment systems. The study focused on multicomponent poisoning conditions involving sulfur together with sodium, calcium, potassium or phosphorus.

Fe-Beta monolith catalysts were aged under simulated exhaust conditions. The catalysts were exposed to hydrothermal treatment and combinations of sulfur with different impurities. Catalyst performance was evaluated through NO<sub>x</sub>, NH<sub>3</sub> and N<sub>2</sub>O conversion measurements, while structural characterization was carried out using DRIFTS, BET, XRD and SEM-EDS analyses.

All impurity treatments reduced catalytic activity compared to the reference (hydrothermally aged) catalyst. Sodium and phosphorus caused the strongest deactivation effects. BET analysis showed a decrease in microporous surface area after impurity exposure, while SEM-EDS mapping revealed non-uniform accumulation of impurity elements within the catalyst layer. These structural changes were linked to reduced active sites and lower catalyst efficiency.

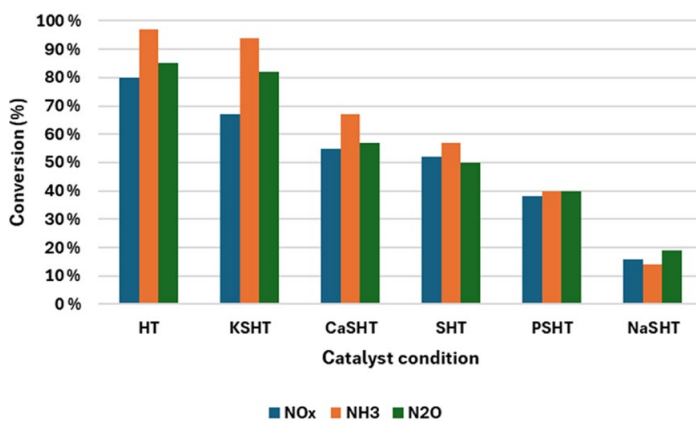


**Figure 1.** Dimensionless temperature distribution in the ullage of the partially filled LH2 tank after P = 0, 1, 2 and 3 (pe-riods of tank motion).

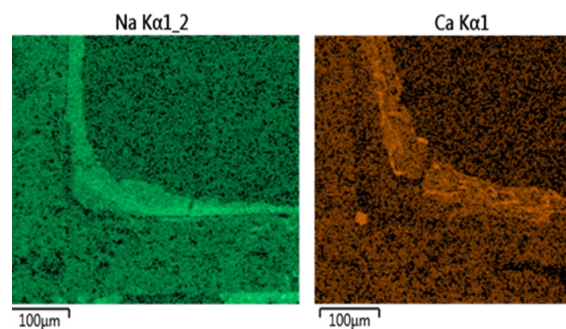


**Figure 2.** SEM-EDS elemental maps showing non-uniform accumulation of impurity elements in the catalyst layer.

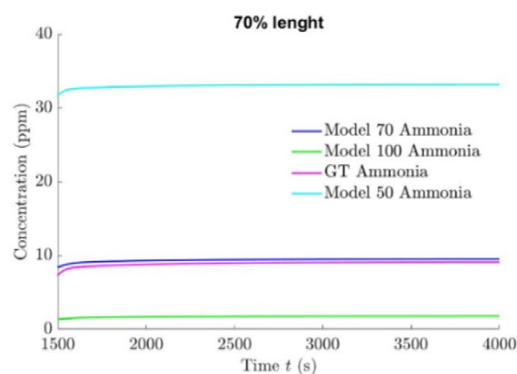
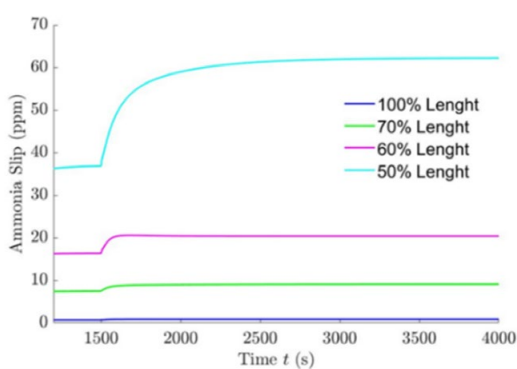
The study demonstrates that biofuel-derived impurities strongly affect NH<sub>3</sub>-SCR catalyst performance by reducing catalytic activity and altering catalyst structure. The findings indicate that impurity accumulation decreases the number of available active sites for SCR reactions, leading to catalyst deactivation.

# State Estimation Applied to SCR Catalyst Aging

**Authors:** Alex Pesu, Jari Böling, Jan Torrkulla, Tahmorees Farjam

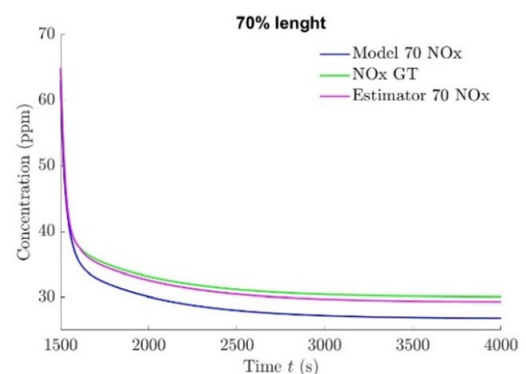
**Keywords:** State estimation, SCR, aftertreatment, Kalman filter, deactivation

Catalyst aging or deactivation is a problem for SCR applications as it will affect the NO<sub>x</sub> reduction performance and required urea dosage. This can be simulated in GT xCHEM software, where a high-level extruded SCR model is used, and catalyst aging is artificially generated by reducing catalyst dimensions in the software parameters by a chosen percentage. As the NO<sub>x</sub> output is controlled (30 ppm) and the same simulation is executed with different simulated deactivation degrees, it is expected that ammonia slip levels increase with more aging, as visualized in the Figure to the left. Therefore, it would be of interest to be able to estimate the catalyst age and how ammonia slip is changing with the level of deactivation.



To enable online state estimation of the SCR, a simple CSTR model is utilized to reduce the computational load. The simplified model consists of three differential equations that describe the ammonia coverage on the catalyst surface in addition to both NO<sub>x</sub>- and ammonia concentrations leaving the SCR. Importantly, the model parameters can be adjusted to generate multiple simple models that each mimic a specific level of aging. In the Figure to the right, there is an example of different adjusted prediction models compared to a 30 percent aged GT xCHEM model, where the similarly aged simple model is closest to the validation model when ammonia slip is evaluated.

The Kalman filter (KF) algorithm is used as the state estimation method. SCR prediction model calculations and system measurements (NO<sub>x</sub> sensor signal) are fused in the Kalman filter to produce more accurate estimates of the NO<sub>x</sub> concentration. In theory also ammonia measurement could be used, but to minimize required sensors it is chosen to only include NO<sub>x</sub> measurement. Therefore, the ammonia slip accuracy depends on the prediction model alone. Due to the nonlinearity of the system a constant gain extended Kalman filter is used. In the last Figure, the NO<sub>x</sub> estimation is compared against the initial prediction of the simple model and the aged GT validation model. The estimator reduces the gap between the initial prediction and the validation model.



# Development of an Electro-Thermal Battery Model and a Novel Battery Management Strategy

**Authors:** Mehdi Zare, Amir-Mohammad Shamekhi, Jaber McBreen, Maciej Mikulski

**Keywords:** Lithium-ion battery; Battery state of health; SOH; Electro-thermal battery modelling; Battery management system

Lithium-ion battery performance, safety, and lifetime are strongly affected by the interaction between electrochemical behaviour, heat generation, and degradation. In this work, an electro-thermal battery model integrated with thermodynamic analysis was developed to evaluate battery thermal behaviour and state of health under operating conditions.

The model combines electrical and thermal battery behaviour with thermodynamic analysis, including reversible and irreversible heat effects. A Kalman filter approach was used for SOC (state of charge) and SOH (state of health) estimation. Battery state of health was evaluated using capacity fade, internal resistance growth, and irreversible entropy generation rate.

Real test data from a Hyundai Sonata were used as the battery current profile to evaluate the thermal response of the battery. The results show the battery temperature behaviour under natural cooling together with the irreversible entropy generation rate. Since the analysis was performed for a hybrid vehicle, the SOC remained nearly constant during the investigation of load profile.

The developed virtual battery model can predict battery thermal behaviour under different cooling conditions, including natural cooling, liquid cooling, and fan cooling. It also supports lifetime prediction under specific load conditions, indicating that the battery may fail after approximately five years or less depending on operating conditions. In addition, a battery management system was developed and implemented to control current and monitor voltage, temperature, and SOC, thereby improving battery performance and operational reliability in real applications. (image 1)

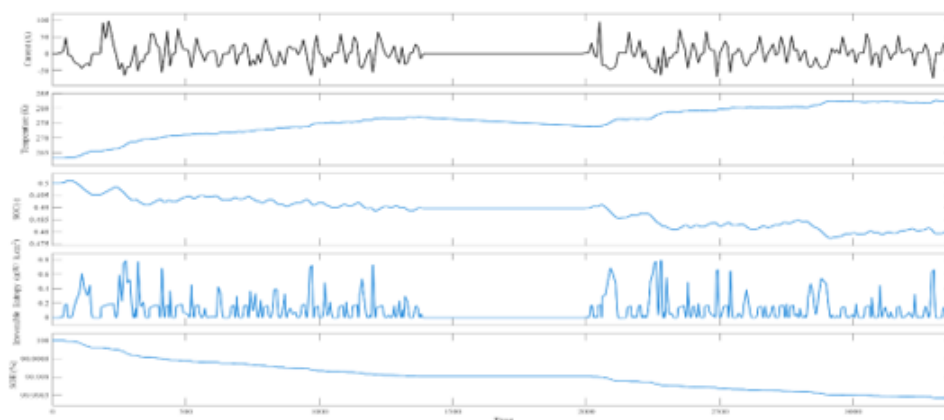


**Image 1.** Real data analysis of battery including load profile, Temperature of battery and SOC and SOH.

# Empirical Modelling of Li Ion Battery Degradation Under Calendar and Cyclic Stress Factors

**Authors:** Muhammad Rehan, Samppa Jenu

**Keywords:** lithium-ion batteries, Calendar ageing, Cyclic ageing, Empirical modelling, Stress factors

This work presents the development of an empirical degradation model for lithium-ion batteries, with a focus on NMC and LFP chemistries. The primary objective is to estimate battery lifetime under operational conditions by considering degradation stress factors.

Battery degradation is represented by calendar and cyclic ageing. Calendar ageing considers capacity fading during idle storage and is modelled as a function of state of charge (SoC), temperature ( $T$ ) and time( $t$ ). Cyclic ageing considers capacity fading during operation and is modelled as a function of temperature ( $T$ ), depth of discharge (DoD), mean state of charge (mSoC), c-rates ( $I_{ch}$ ,  $I_{disch}$ ) and the number of full equivalent cycles (FEC) as presented in the model equations.

The model is developed using a large dataset compiled from published experimental lifetime studies for both chemistries. The methodology includes data collection, preprocessing, clustering, normalization, curve fitting, and model integration. To remove the effect of differences in absolute lifetime due to variability in cell, manufacturer, and test conditions, normalization is applied to retain the relative influence of individual stress factors. Data clustering is used to isolate the effect of specific stress factors while keeping other stress factors constant.

Based on trends observed in the dataset, exponential functions are used to define the degradation due to SoC and temperature for calendar ageing. For cyclic ageing, exponential functions are used for DoD and C-rates, while Gaussian functions represent fading for temperature and mSoC. These stress-factor functions are combined into a lifetime model. The state of health (SoH) is defined as the remaining capacity due to both calendar and cyclic degradation.

The modelling activity indicate that temperature is the dominant factor in both calendar and cyclic degradation. Elevated temperature and high storage SoC accelerate calendar ageing, while cyclic ageing is observed to be minimum for small DoD at 50% mSoC, 25 °C, and low C-rates. The model considers calendar ageing during idle periods, whereas cyclic ageing during active operation and can be implemented for a use case with rain flow counting algorithm for FEC.

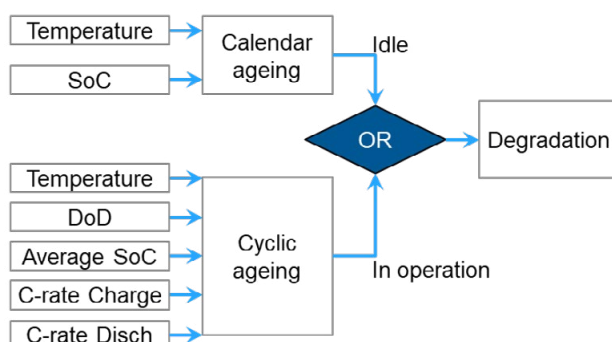


**Figure 1.** The illustration of model workflow

The developed model is represented with the following equations.

$$SoH = 1 - (\Delta SoH_{cal} + \Delta SoH_{cyc})$$

$$\Delta SoH_{cal} = \frac{(1 - EoL) \times t}{\lambda_{\theta}^{cal} \times \lambda_T^{cal} \times \Gamma_{ref}^{cal}}$$

$$\Delta SoH_{cyc} = \frac{(1 - EoL) \times FEC}{\lambda_{\delta}^{cyc} \times \lambda_T^{cyc} \times \lambda_{\theta}^{cyc} \times \lambda_{I_{ch}}^{cyc} \times \lambda_{I_{disch}}^{cyc} \times \Gamma_{FEC}^{cyc}}$$

Symbols details are below:

Symbol	Details
$SoH$	State of health in percentage
$\Delta SoH_{cal}$	Calendar degradation
$\Delta SoH_{cyc}$	Cyclic degradation
$EoL$	End of life (80% SoH)
$t$	storage time in days for calendar ageing
$\lambda_{\theta}^{cal}$	Calendar lifetime function for state of charge
$\lambda_T^{cal}$	Calendar lifetime function for temperature
$\Gamma_{ref}^{cal}$	Reference calendar life in day
$FEC$	Full equivalent cycles
$\lambda_{\delta}^{cyc}$	Cyclic lifetime function for depth of discharge
$\lambda_T^{cyc}$	Cyclic lifetime function for temperature
$\lambda_{\theta}^{cyc}$	Cyclic lifetime function for mean state of charge
$\lambda_{I_{ch}}^{cyc}$	Cyclic lifetime function for charging c-rate
$\lambda_{I_{disch}}^{cyc}$	Cyclic lifetime function for discharging c-rate
$\Gamma_{FEC}^{cyc}$	Reference cyclic life in full equivalent cycles

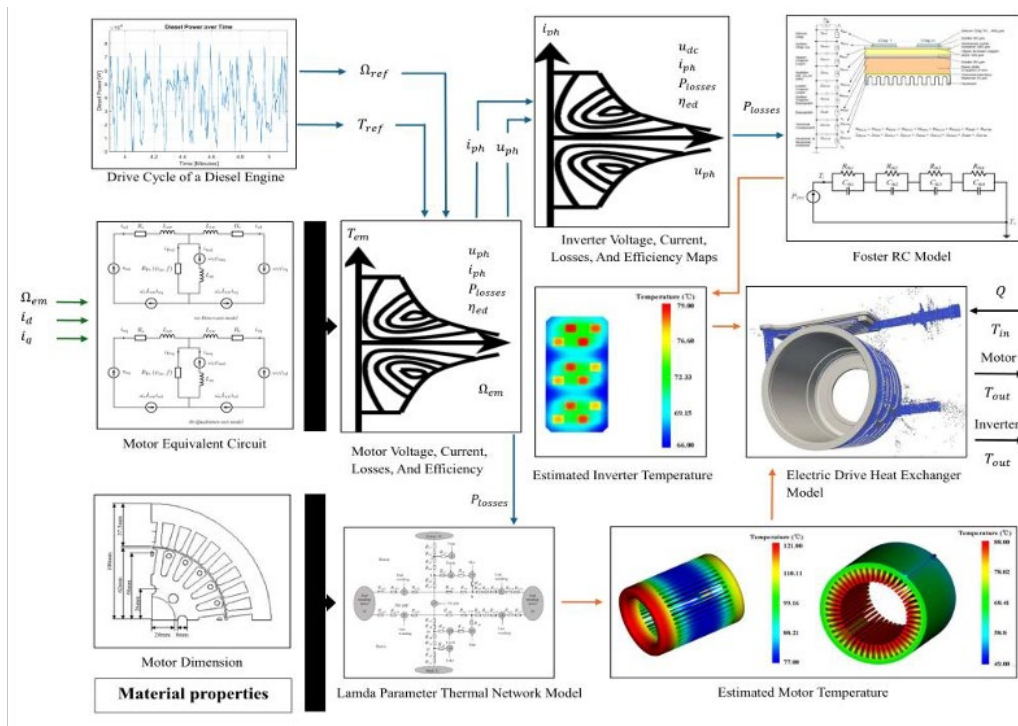
# Modelling of a Liquid-Cooled Electrical Drive

**Authors:** Pasi Peltoniemi, Sofiane Abdelaziz

**Keywords:** Power losses and thermal estimation of electric drive, PMSM, IM, Inverter, Reduced model, Equivalent circuit analysis, Lambda parameter thermal network, Forster model

## Background

Despite the benefits of hybrid electric NRRMs, they operate under highly dynamic and non-standardized load cycles, characterized by fluctuating torque, speed, and environmental conditions. This variability complicates both performance prediction and thermal management design. That becomes especially critical because the electric drive, including motor, inverter, and associated systems, generates substantial heat under high power density conditions. If not accounted for, these causes elevate temperatures that degrade performance, reduce efficiency, and shorten the component lifespan of the machine.



## Challenges

The main challenges in modelling a liquid-cooled electric drive arise from the complex electro-thermal phenomena under dynamic operating conditions: losses originate from the motor and inverter and vary with speed and torque, while temperature simultaneously influences these losses through parameters such as electrical resistance, creating a strong coupling effect. At the same time, modelling must balance accuracy and computational efficiency, since high-fidelity methods such as FEM or CFD are too slow for drive-cycle simulations, whereas simplified approaches, including equivalent circuit analysis for loss estimation and lumped-parameter thermal networks (LPTN), introduce approximations in spatial temperature distribution and rely on empirical parameters that must be estimated with limited inputs. These challenges are further amplified by highly variable load profiles and operating conditions, which complicate validation and limit the ability to generalize the model.

# Passive Thermal Management and Thermal Modelling of Li-Ion Cells

**Authors:** Shruthi Meda, Soroush Mostafaie, Pertti Kauranen

**Keywords:** PCM, lumped model, NRMM

## Abstract

Demanding operating conditions of NRMM batteries increase their internal temperatures, highlighting the need for more precise thermal analysis and management systems. Two theses were combined to link passive thermal management of prismatic NRMM battery modules with cell-level thermal modelling of NCA batteries.

The PCM based passive cooling method was found to reduce the peak temperatures of the module from 37 to 34 and provide more uniform temperatures within the battery module. The lumped thermal model of 21700 NCA cells was able to predict the temperature behaviour of the cells, with the averaged-SOC at constant-OCV method providing more accurate results. Together, these studies provide more accurate prediction of thermal behaviour and support the development of safer battery systems.

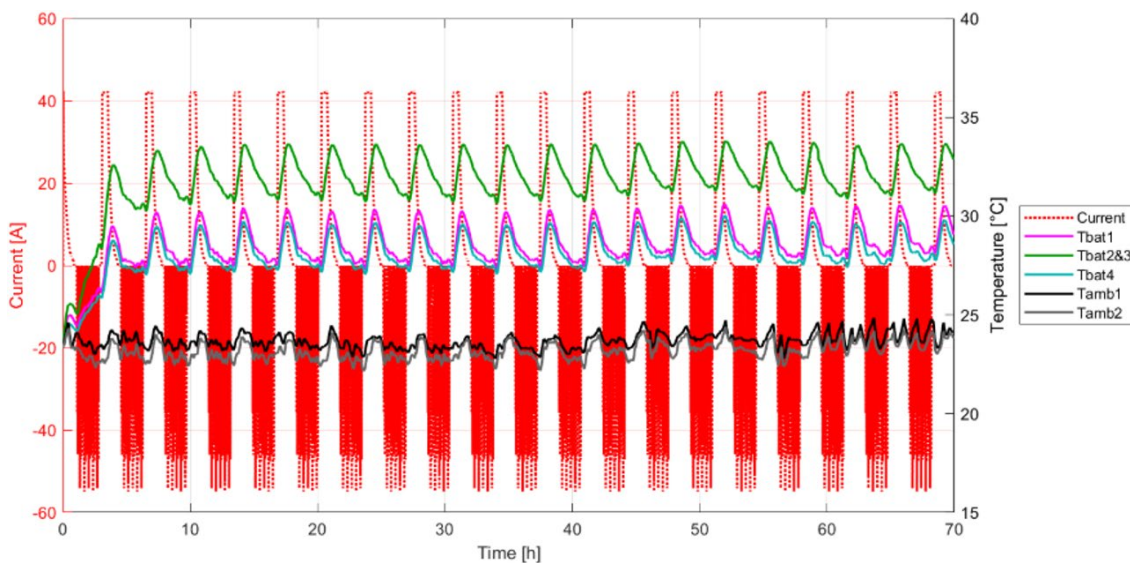


**Figure 1.** Current and temperature profile for 20 NRTC Cycles

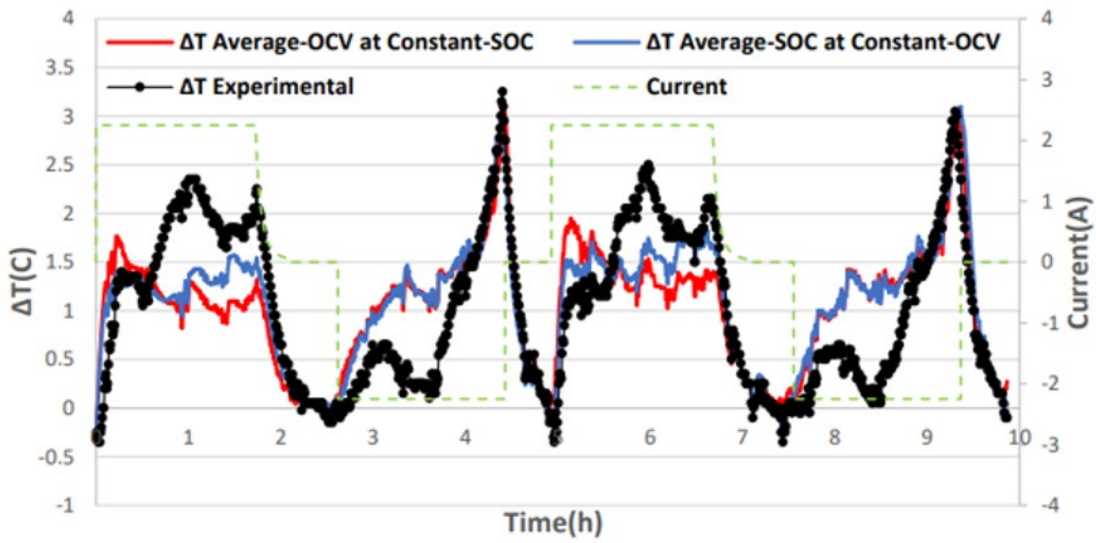


Figure 2. Thermal Model Validation at 0.5C



## References:

- Auvinen, K.; Kaminen, K.; Karhinen, S.; Rekola, A.; Pelkonen, J.; Child, M.; Kärhä, K.; Rantsi, J.; Ihonen, J.; Suomalainen, E.; Hyrynen, J.; Pesonen, J., and Rasi, S. 2025. Poliittikkatoimet liikkuvien työkoneneiden puhtaan siirtymän edistämiseksi. In Finnish. Available: <http://hdl.handle.net/10138/593784>
- Kanger, L., Sovacool, B. K., Noorkõiv, M. 2020. Six Policy Intervention Points for Sustainability Transitions: A Conceptual Framework and a Systematic Literature Review. *Research Policy* 49 (7): 104072. <https://doi.org/10.1016/j.respol.2020.104072>
- Karhinen, S. 2026. Näkökulmia päästövähennystoimien kustannusvaikuttavuuteen ja ohjauskeinoihin Suomessa. In Finnish. <http://hdl.handle.net/10138/629334>
- Ministry of the Environment. 2025. Annual Climate Report 2025. In Finnish. Available: <https://urn.fi/URN:ISBN:978-952-361-686-8>
- Rasmussen & Williams (2006); Settles (2009); Marchant & Ramos (2014); Bishop (2006); Maciejowski (2002).
- Sirviö, K.; Kaivosoja, J.; Nuortila, C.; Wang-Alho, H.; Niemi, S.; Ovaska, T. B20 Fuel Compatibility with Steels in Case of Fuel Contamination. *Energies* 2023, 16, 5933. <https://doi.org/10.3390/en16165933>
- Wang-Alho, H.; Sirviö, K.; Nuortila, C.; Kaivosoja, J.; Mikulski, M.; Niemi, S. Compatibility of Methanol-Hydrotreated Vegetable Oil Blends with Chosen Steels and Aluminum. *Energies* 2024, 17, 3423. <https://doi.org/10.3390/en17143423>
- Kaivosoja, J.; Sirviö, K.; Nuortila, C.; Niemi, S. Effects of Fuel Hydrochloric Acid Contamination on Selected Metals. *J. Mar. Sci. Eng.* 2024, 12, 776. <https://doi.org/10.3390/jmse12050776>
- Sieranen, I. 2025. Fuel-induced corrosion: Analysis of temperature effect on carbon steel immersed in various fuels. Master thesis. *Energy Technology, Smart Energy*. University of Vaasa. Available: <https://urn.fi/URN:NBN:fi-fe2025022514348>
- Nuortila C.; Sirviö, K.; Kaivosoja, J.; Sieranen, I.; Wang-Alho, H.; Balogun, F.; Niemi, S. Corrosion study on carbon steel immersed in alternative fuels. Poster in CIMAC congress, Zürich, May 19-23, 2025.
- Yong H.; Zezhou W.; Hui C.; Yue L.; Xin L.; Shaobin W.; Wei H.; Cheng S. Importance of the autoclave testing parameters on the initial stage of corrosion under CO<sub>2</sub>-containing geothermal environments, *Corrosion Communications*, 2024. <https://doi.org/10.1016/j.corcom.2023.10.004>.
- Yong C.; Ziming W.; Qun L.; Yingwei S.; Kaihui D. Corrosion Behavior of Marine Engine Piston 16CrMo Alloy Steel in the Artificial Methanol Fuel Combustion Product Environment, *Materials Today Communications*, 2025. <https://doi.org/10.1016/j.mtcomm.2025.114417>.



**Flexible Clean  
Propulsion  
Technologies**

## **Contact details**

**Diana Ibraheem**  
diana.ibraheem@uwasa.fi  
+358 29 449 8563

**Merja Kangasjärvi**  
merja.kangasjarvi@uwasa.fi  
+358 29 449 8205